Triple oxygen isotope composition of CO_2 in the upper troposphere and stratosphere

Getachew Agmuas Adnew[1,*], Gerbrand Koren[2], Neha Mehendale[1,**], Sergey Gromov[3], Maarten Krol[1,4], and Thomas Röckmann[1]

[1]Institute for Marine and Atmospheric research Utrecht (IMAU), Physics Department, Science Faculty, Utrecht University, Princetonplein 5, 3584 CC Utrecht, the Netherlands
[2]Copernicus Institute of Sustainable Development, Utrecht University, Princetonlaan 8a, 3584 CB Utrecht, the Netherlands
[3]Max Planck Institute for Chemistry, Hahn-Meitner-Weg 1, 55218 Mainz, Germany
[4]Meteorology and Air Quality, Wageningen University, Wageningen, the Netherlands
[*]now at the Terrestrial Ecosystem Analysis Group, Institute of Geography, people and processes, Department of Geosciences and Resource management, Science Faculty, University of Copenhagen, Øster Voldgade 10 1350 Copenhagen K, Copenhagen, Denmark
[**]now at Institute for Environmental Physics, University of Bremen, Otto-Hahn-Allee 1, 28359,Bremen, Germany
Correspondence: Getachew Agmuas Adnew (gaa@ign.ku.dk)

Abstract. High precision measurements of the triple oxygen isotope composition of CO_2 ($\Delta'^{17}O$) can be used to estimate biosphere-atmosphere exchange of CO_2, the residence time of tropospheric CO_2 and stratosphere-troposphere exchange. In this study, we report measurements of the $\Delta'^{17}O(CO_2)$ from air samples collected during two aircraft based programs, CARIBIC and StratoClim. CARIBIC (Civil Aircraft for the Regular Investigation of the atmosphere based on an Instrument Container)

5 provided air samples from numerous transcontinental flights in the upper troposphere/lower stratosphere region. StratoClim (Stratospheric and upper tropospheric processes for better climate predictions) conducted intensive campaigns with the high-altitude aircraft M55 Geophysica during the Asian Summer Monsoon Anticyclone (ASMA), providing air samples from altitudes up to 21 km.

Using high precision $\Delta'^{17}O$ measurements of the CARIBIC samples, we show that the N_2O-$\Delta'^{17}O$ correlation, previously

10 observed in the stratosphere, extends to the upper troposphere. Moreover, we found no significant spatial or hemispheric differences in $\Delta'^{17}O(CO_2)$ for the upper tropospheric samples collected during the CARIBIC program. However, in many of the StratoClim samples, with significant stratospheric contributions, we observed a much lower N_2O-$\Delta'^{17}O$ slope compared to CARIBIC samples and previous publications. This deviation is attributed to change in eddy diffusion above the tropopause within the ASMA, confirming previously published model calculations. These samples provide the first experimental evidence

15 that differences in vertical mixing/transport can lead to significantly different N_2O-$\Delta'^{17}O$ slopes. High precision $\Delta'^{17}O$ measurements can identify ejections of tropospheric air into the stratosphere based on the slope of the N_2O-$\Delta'^{17}O$ correlation, as both tracers have chemical lifetimes longer than their transport times.

Furthermore, we use the $\Delta'^{17}O$ measurements from the lower stratosphere and the upper troposphere to estimate global stratospheric production and surface removal of the isotope tracer $\Delta'^{17}O$. The removal estimate is then used to derive an

20   independent estimate of global vegetation exchange of CO_2, confirming earlier estimates based on surface level $\Delta'^{17}O$ measurements.

1   Introduction

Measurements of the isotope composition of CO_2 ($\delta^{13}C$ and $\delta^{18}O$, see definition below) are used in many ways to understand

25   sources and sinks of CO_2 in the global carbon cycle (Farquhar et al., 1993; Welp et al., 2011; Cuntz et al., 2003b; Ciais et al., 1997a, 1995). The flux estimates of CO_2 from the terrestrial biosphere are poorly constrained in current carbon cycle models (Piao et al., 2013). By using $\delta^{13}C$ it is possible to differentiate between the ocean sink and biosphere activity. However, distinguishing respiration, photosynthesis and combustion signals using $\delta^{13}C$ of CO_2 is impossible (Ciais et al., 1995). To address this challenge, $\delta^{18}O$ of CO_2 is a valuable tool for distinguishing respiration from photosynthesis. The $\delta^{18}O$ value of

30   CO_2 is higher during photosynthesis than during respiration due to isotope exchange of CO_2 with isotopically different leaf water and soil water pools, as leaf water typically has a higher $\delta^{18}O$ value than soil water (Ciais et al., 1997a, b; Welp, 2011; Farquhar et al., 1993; Cuntz et al., 2003a, b; Francey and Tans, 1987; Yakir, 2020).

    One of the limitations of using $\delta^{18}O$ of CO_2 to distinguish photosynthesis and respiration is the oxygen isotope exchange of CO_2 with liquid water in surface water bodies or vegetation, since this isotope exchange affects $\delta^{18}O$ of CO_2, without

35   contributing to a net flux. Numerous equilibrium and kinetic effects can alter the $\delta^{18}O$ value of water and other molecules (Cuntz et al., 2003a, b; Peylin et al., 1999). Importantly, the isotopic composition of leaf water at the CO_2-H_2O exchange site in the mesophyll is not well understood, primarily due to fractionation associated with evaporation, transport, and diffusion ~~(Adnew et al., 2020a, 2021, 2023; Gan et al., 2002; Cousins et al., 2006; Song et al., 2015; Landais et al., 2006; Cernusak et al., 2016; He~~ (Adnew et al., 2020b, 2021, 2023; Gan et al., 2002; Cousins et al., 2006; Song et al., 2015; Landais et al., 2006; Cernusak et al., 2016; He

40   . These unknown physico-chemical fractionation processes introduce large uncertainty into estimates of gross fluxes of CO_2 when using $\delta^{18}O$ as quantitative tracer. This uncertainty can potentially be reduced using the triple oxygen isotopic composition of CO_2, $\Delta'^{17}O$ (see equation 4), which is a combination of the $\delta^{17}O$ and $\delta^{18}O$ isotopic composition ~~(Hoag et al., 2005; Koren et al., 2019; A~~ (Hoag et al., 2005; Koren et al., 2019; Adnew et al., 2020b).

    Stratospheric CO_2 has a high $\Delta'^{17}O$ value, i.e., $\Delta'^{17}O \gg 0$, due to isotope exchange with $O(^1D)$ produced from O_3 photol-

45   ysis (Thiemens et al., 1991, 1995b; Lyons, 2001; Lämmerzahl et al., 2002; Thiemens, 2006; Kawagucci et al., 2008; Wiegel et al., 2013; Yung et al., 1991b, 1997b; Shaheen et al., 2007). The main sink for this higher $\Delta'^{17}O$ signal of CO_2 is isotope exchange with leaf, soil and ocean water at the Earth's surface, after $\Delta'^{17}O$ enriched CO_2 has re-entered the troposphere via the large-scale Brewer-Dobson circulation and synoptic eddy diffusion (Boering et al., 2004b; Thiemens et al., 2014; Liang and Mahata, 2015; Francey and Tans, 1987). With the exception of stratospheric CO_2, $\Delta'^{17}O$ variations in na-

50   ture are much smaller compared to $\delta^{18}O$ variations, and are better defined, as conventional biogeochemical processes fol-

low a well-defined three-isotope fractionation slope (Barkan and Luz, 2005, 2007, 2012; Landais et al., 2006; Angert et al., 2004, 2003). Furthermore, the triple oxygen isotope fractionation slopes for specific processes are independent of the source water isotope composition, insensitive to temperature, and process-specific (Landais et al., 2006; Hofmann et al., 2012). As a result, $\Delta'^{17}O$ is less affected by the numerous physico-chemical fractionation processes mentioned above, and may

55   provide an additional constraint for quantifying the gross fluxes of the terrestrial carbon cycle than measuring $\delta^{18}O$ alone ~~(Koren et al., 2019; Hoag et al., 2005; Liang et al., 2017a, 2023; Hofmann et al., 2017; Adnew et al., 2020a; Thiemens et al., 2014)~~ (Koren et al., 2019; Hoag et al., 2005; Liang et al., 2017a, 2023; Hofmann et al., 2017; Adnew et al., 2020b; Thiemens et al., 2014) .

In addition to quantifying the gross fluxes of the terrestrial carbon cycle, $\Delta'^{17}O$ can provide useful information for concern-

60   ing stratospheric intrusions (Liang and Mahata, 2015; Steur et al., 2024), stratosphere-troposphere exchange, (Boering et al., 2004b; Luz et al., 1999), atmospheric transport and chemistry in the mesosphere and stratosphere (Liang et al., 2007b, 2008), combustion processes (Laskar et al., 2016; Horváth et al., 2012) and for estimating the residence time of CO_2 in the troposphere (Liang et al., 2017b; Laskar et al., 2019; Hoag et al., 2005).

High precision measurements of $\Delta'^{17}O(CO_2)$ are particularly interesting in the tropical upper troposphere/lower most strato-

65   sphere region, which is remote from the sources and sinks. Therefore, $\Delta'^{17}O(CO_2)$ can be used to study the influence of the stratosphere-troposphere exchange on the variations and dynamics of $\Delta'^{17}O$ and its correlation with other long- and short-lived trace gases. Additionally, these measurements may be valuable for using $\Delta'^{17}O$ as a tracer to quantify gross fluxes of CO_2, as this region links the stratosphere, where $\Delta'^{17}O$ of CO_2 is produced, to the troposphere, where $\Delta'^{17}O$ of CO_2 is "washed out". Furthermore, it is interesting to investigate whether $\Delta'^{17}O$ varies spatially in the upper troposphere and whether it is possible

70   to detect large scale dynamic phenomena that happen in the Asian Summer Monsoon Anticyclone (ASMA). The Monsoon circulation system has a large variability in its spatial extent and the ASMA can reach the Mediterranean, North-east Africa and East Asia (Annamalai and Slingo, 2001; Garny and Randel, 2013; Pan et al., 2016; Vogel et al., 2019).

Here we present high-precision measurements of $\Delta'^{17}O(CO_2)$ from a total of 85 air samples collected in the upper troposphere and stratosphere as part of the CARIBIC and StratoClim aircraft air sampling projects. We investigate the spatial

75   distribution (horizontal and vertical) of $\Delta'^{17}O(CO_2)$, signals associated with the ASMA, and refine previous estimates of the net stratosphere-troposphere flux of $\Delta'^{17}O(CO_2)$ and constraints on surface CO_2 emissions.

2   Materials and Method

2.1   Definitions and notation

Variations in isotopic abundance are reported as deviations of a heavy-to-light isotope ratio in a sample relative to a reference

80   material (Eq. 1). For oxygen the reference material is Vienna Standard Mean Ocean Water (VSMOW) whereas for carbon the reference material is Vienna Pee Dee Belemnite (VPDB). Since isotope variations are small, they are usually reported in per

mill (‰) in delta notation.

$$\delta^x = \frac{{}^x R_{sam}}{{}^x R_{std}} - 1 \tag{1}$$

where x can be 13, 17 and 18 (for ${}^{13}C$, ${}^{17}O$ and ${}^{18}O$, respectively). The indices *sam* and *std*, stand for sample and standard, respectively and R is the ratio between the heavy isotope and the light isotope of the respective element, for instance for ${}^{13}C$ and ${}^{18}O$, ${}^{13}R = \frac{{}^{13}C}{{}^{12}C}$ and ${}^{18}R = \frac{{}^{18}O}{{}^{16}O}$, respectively. The variations in $\delta^{17}O$ and $\delta^{18}O$ are closely related during most physico-chemical fractionation processes according to Eq.2 (Matsuhisa et al., 1978; Young et al., 2002).

$$\left(\frac{{}^{18}R_{sam}}{{}^{18}R_{std}} \right)^{\theta_p} = \frac{{}^{17}R_{sam}}{{}^{17}R_{std}} \tag{2}$$

The exponent θ_p denotes a three isotope slope that occurs from a single process. Equation 2 can be expressed in δ- notation as:

$$ln(\delta^{17}O + 1) - \theta_p \times ln(\delta^{18}O + 1) = 0 \tag{3}$$

The deviation of the left hand side of equation 3 from zero is defined as $\Delta'^{17}O$ (Eq. 4).

$$\Delta'^{17}O = ln(\delta^{17} + 1) - \lambda_{ref} \times ln(\delta^{18}O + 1) \tag{4}$$

where the process-dependent exponent θ_p has been replaced by a three-isotope reference slope λ_{ref}. Note that the choice of λ_{ref} is arbitrary since in nature isotopic compositions rarely reflect fractionation from a single process, but instead integrate multiple fractionating processes and several three-isotope values (Adnew, 2020; Barkan and Luz, 2005, 2007, 2012; Angert et al., 2004). For most natural processes λ_{ref} ranges from 0.5 to 0.5305 (Thiemens, 2006; Matsuhisa et al., 1978; Young et al., 2002; Cao and Liu, 2011; Thiemens et al., 1991; Kaiser, 2008) with some exceptions (Adnew et al., 2022; Hayles et al., 2017; Hayles and Killingsworth, 2022). In this study we use a λ_{ref} value of 0.528, the value associated with meteoric water (Meijer and Li, 1998; Luz and Barkan, 2010).

2.2 Sampling

Air samples were collected from the upper troposphere and stratosphere during two different international projects, CARIBIC and StratoClim, which are shortly described below. Figure 1 shows the geographical coordinates of the sampling locations for the samples measured in this study.

2.2.1 CARIBIC samples

In the CARIBIC project (Civil Aircraft for the Regular Investigation of the atmosphere Based on an Instrument Container, CARIBIC, https://www.caribic-atmospheric.com/), samples were collected using a Boeing 767 aircraft (LTU, Germany). The flights operated at typical commercial cruising altitude between 9 and 12 km, i.e., which is the upper troposphere-lower

stratosphere region at higher latitudes and the upper troposphere region in the mid latitudes and tropics (Assonov et al., 2010)

110 . The details of the CARIBIC instrument container are described in Brenninkmeijer et al. (1999). The payload of the flights before 2003 included large stainless steel canisters for collecting whole air samples (WAS) (sample size $\approx$ 340 L STP) at several locations along the flight path. On a single flight 12 discrete samples were collected. Each sample collection took about 20 min which corresponds to a horizontal distance of 250 km (Brenninkmeijer et al., 1999). The samples collected are relatively dry since the ambient temperature was always below -30 °C and the relative humidity was about 0.44 % at 20 °C

115 (Assonov et al., 2009b). The air samples were processed soon after they returned to the Division of Atmospheric Chemistry, Max Planck Institute for Chemistry, Mainz, Germany (Pupek et al., 2005). The processing included the extraction of CO_2 and CO for isotope analysis, including radiocarbon (Brenninkmeijer, 1993; Assonov et al., 2009b) as well as measurement of several other trace gases including N_2O, CH_4 and SF_6 (Brenninkmeijer et al., 1999). The CARIBIC container was also equipped with an automated in-situ analyzer for O_3 (UV absorption), CO (gas chromatography (GC)) and other parameters

120 (Brenninkmeijer et al., 1999). In this study we measured the $\Delta'^{17}O$ value of 50 CARIBIC samples.
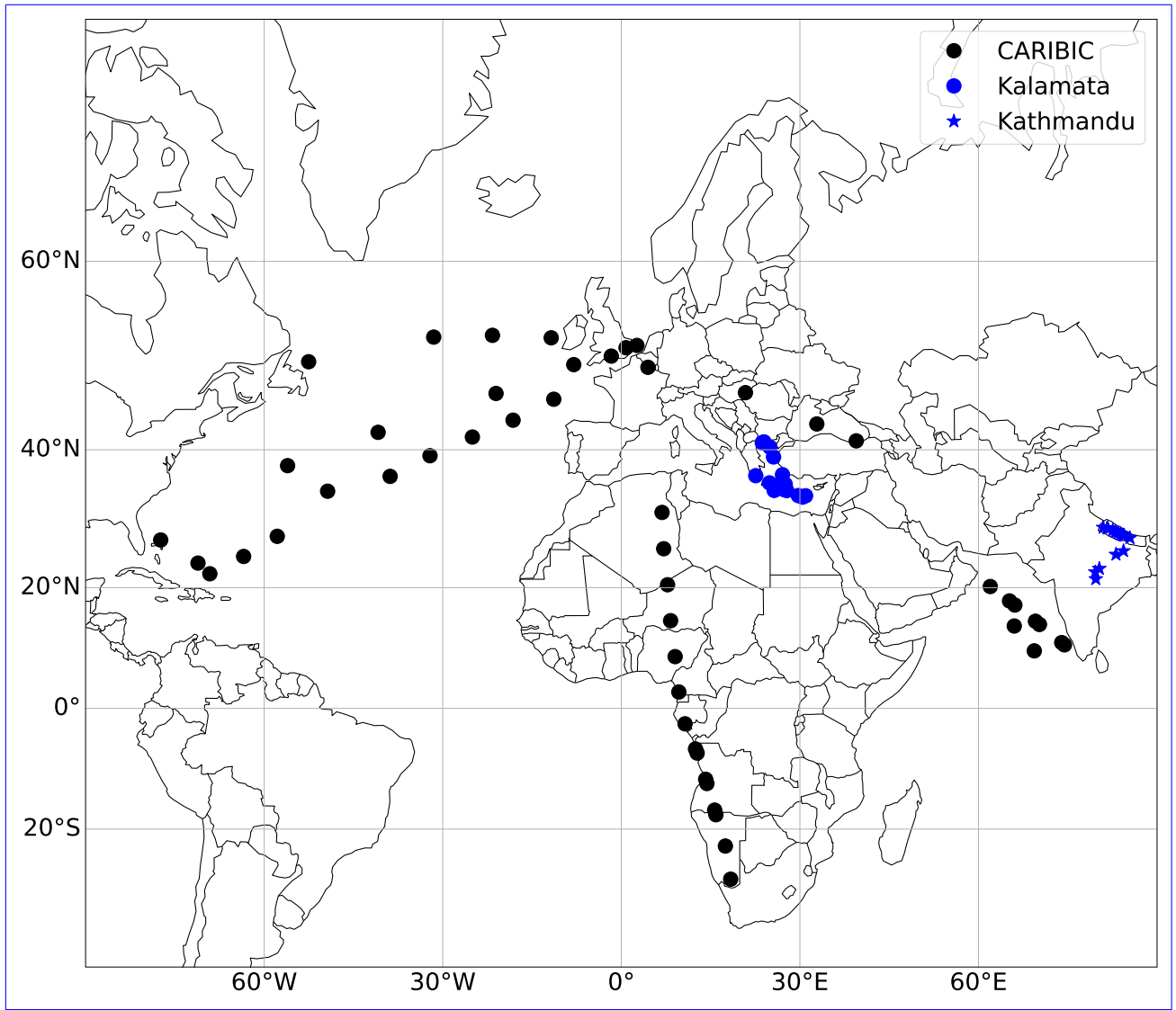
2.2.2 StratoClim samples

35 additional air samples were collected on the high-altitude M55 Geophysica aircraft during two campaigns of the StratoClim project (https://www.stratoclim.org/) (Stefanutti et al., 1999; Cairo et al., 2010) in 2016 and 2017. In 2016, three flights were conducted over the Mediterranean region from Kalamata, Greece (37°2′N and 22°7′E) between August 30 and 6 September

125 and eight flights were conducted in 2017 over the Indian subcontinent from Kathmandu, Nepal (27°46′N and 85°16′E) between 27 July and 10 August. The whole air sampler of the Institute for Marine and Atmospheric research Utrecht (IMAU), Utrecht University was used to compress air into 2 L pre-evacuated stainless-steel canisters (Kaiser et al., 2006). We analysed 16 samples from the 2016 flights and 19 samples from the 2017 flights (Table S3). Further details on sample collection using the Geophysica aircraft can be found in Kaiser et al. (2006) and Stefanutti et al. (1999).

130 ### 2.3 Extraction of CO_2

For the StratoClim samples, the CO_2 was extracted from the whole air samples using a cryogenic extraction system developed at Utrecht University (Adnew et al., 2020b, 2023). The extraction system was made of electropolished stainless steel and has four traps. The first two traps remove moisture and condensable organics at dry ice temperature whereas the third and fourth traps were used to collect CO_2 at liquid nitrogen temperature. The extraction was performed at a flowrate of 55 mL/min.

135 For the CARIBIC samples, the CO_2 had previously been extracted at the Max Planck Institute for Chemistry, Mainz, as described in Assonov et al. (2009b) and Pupek et al. (2005). Two "Russian Doll" cryogenic traps (Brenninkmeijer and Röckmann, 1996; Br immersed in liquid nitrogen trapped all condensable gases including CO_2, N_2O, H_2O and most organics. After pumping out non-condesables, the traps were slowly heated and the evolving CO_2 and N_2O was trapped in a U-trap cooled with liquid nitrogen while the H_2O remained trapped in the Russian Doll Traps. The collected CO_2 was further dried using P_2O_5 and

140 flame-sealed in clean vials made of borosolicate glass (Assonov et al., 2009b; Pupek et al., 2005).

Figure 1. Geographical location of the CARIBIC (black markers), StratoClim2016 (blue circles) and StratoClim2017 (blue stars) air samples measured in this study. Upper tropospheric CARIBIC samples are categorized based on the geographical location where they are collected. These categories include Southern Hemisphere samples, Northern Hemisphere samples, African samples (longitude between 7° and 45°), Asian samples (longitude > 45°), and American samples (longitude < 0°).

2.4 Measurement of $\delta^{13}C$, $\delta^{18}O$ and $\Delta'^{17}O$ of CO_2

The $\delta^{18}O$ and $\delta^{13}C$ values presented below were measured using a Delta^{PLUS} V isotope ratio mass spectrometer (ThermoScientific, Germany) in dual inlet mode at Utrehct University. The interference of N_2O was corrected using: $\delta^{18}O = \delta^{18}O_{Measured} + \frac{[N_2O]}{[CO_2]}(\frac{347}{1000})$ and $\delta^{13}C = \delta^{13}C_{Measured} + \frac{[N_2O]}{[CO_2]}(\frac{250}{1000})$ (Friedli and Siegenthaler, 1988; Sirignano et al., 2004). Figure 2 shows a comparison

of the the $\delta^{18}O$ and $\delta^{13}C$ of CO_2 of CARIBIC samples measured in this study with those previously measured at the Max-Planck-Institute for Chemistry and reported in Assonov et al. (2009b, a, 2010).
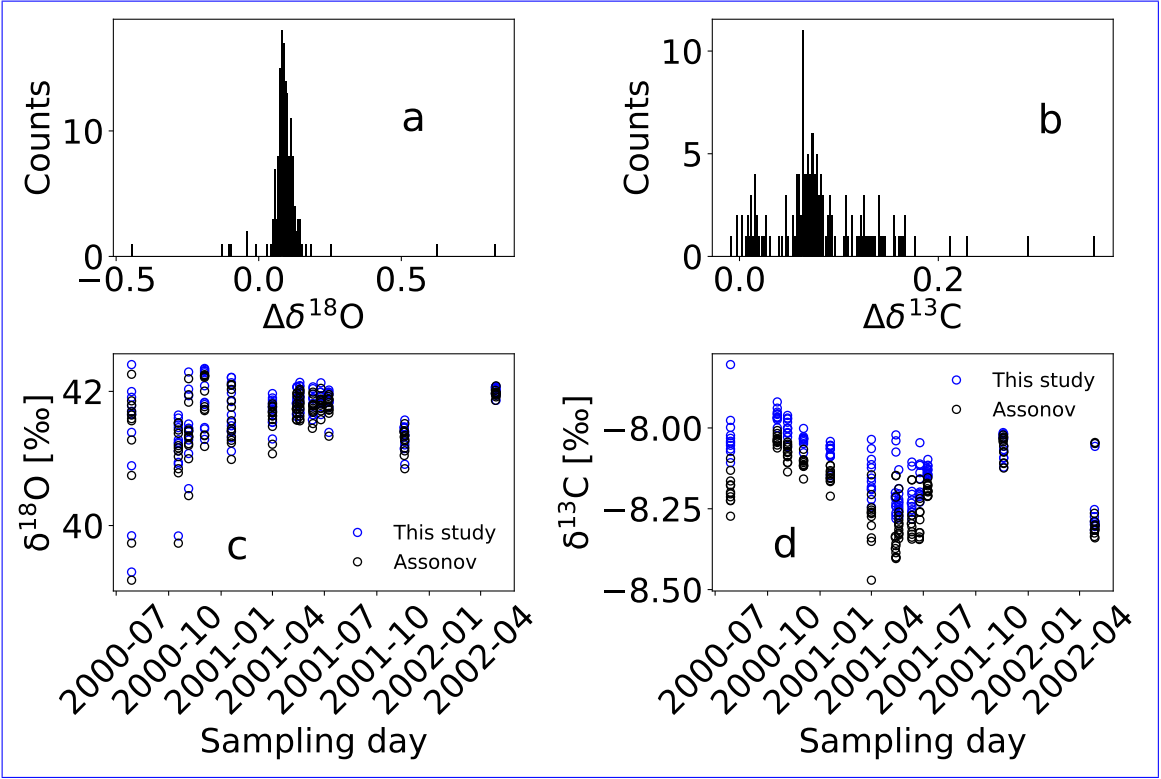
Figure 2. The $\delta^{18}O$ and $\delta^{13}C$ of CARIBIC samples and comparison with values published in Assonov et al. (2009b, a, 2010).

The $\delta^{18}O$ values measured in this study are systematically higher compared to the measurement by Assonov et al. (2010) by 0.096 ± 0.008 ‰. For $\delta^{13}C$ values, our measurement is also higher by 0.089 ± 0.011 ‰. The reported error is the 95 % confidence limit (standard error of the mean multiplied by Student's t-factor). The tight distribution of differences is of the order of the measurement precision, which suggests that the isotopic composition of the samples remained stable during long-term storage in borosilicate glass vials and that the mean offset is due to scale differences. These observed offsets are consistent with the scale uncertainty reported by Assonov et al. (2009a) and better than typical inter-laboratory uncertainties (Levin et al., 2007).

The $\Delta'^{17}O$ of the CO_2 was determined using the CO_2-O_2 exchange method (Adnew et al., 2019, 2022, 2023; Barkan et al., 2015) at Utrecht University. Equal amounts of CO_2 sample and the laboratory reference O_2 (with known isotopic composition) were allowed to exchange isotopes for 2 hours in a quartz reactor at 750°C in the presence of platinum sponge at the bottom of the reactor. After the reaction, the mixture was passed through a liquid nitrogen-cooled trap to condense the CO_2 and the O_2 was collected in a separate trap on 3 pellets of 5Å molecular sieve (1.6mm, Sigma-Aldrich, USA) at liquid nitrogen temperature. The O_2 was then transferred to the bellows of the dual inlet system of a $Delta^{PLUS}$ V isotope ratio mass

spectrometer (ThermoFisher Scientific, Germany) and measured for its isotope composition. The $\Delta^{'17}O$ value of the original CO_2 was calculated from the change in the isotopic composition of the non-reacted and reacted O_2, and knowledge of the precise steady-state O_2-CO_2 isotope fractionations (Adnew et al., 2019; Barkan et al., 2015). The precision of the CO_2 isotope measurements was 0.007 ‰, 0.03 ‰ and 0.008 ‰ for $\delta^{13}C$, $\delta^{18}O$ and $\Delta^{'17}O$ respectively (Adnew et al., 2019, 2020b, 2023)

2.5   Calculation of net isotope flux from stratosphere to troposphere

The isotopic composition of CO_2 in the upper stratosphere and mesosphere provides a unique tool to study atmospheric transport and chemistry (Boering et al., 2004a; Liang et al., 2007a, 2008). The $\Delta^{'17}O(CO_2)$ is primarily modified by $O(^1D)$, which is produced photochemically by O_3 photolysis. However, the relevant isotope effects occurring in the stratosphere are still not yet well enough (Wiegel et al., 2013; Liang et al., 2007b, 2008). Nevertheless, an empirical estimate of the isotope flux from the stratosphere can be derived from measurements near the tropopause, like the ones presented here. As described in detail by Plumb and Ko (1992) and Plumb (2007), gases that are chemically long-lived relative to vertical and quasi-horizontal transport time scales exhibit compact correlations in the stratosphere, and the slope of the observed correlation between the two tracers is equal to the ratio of their net vertical fluxes. Following this approach, Luz et al. (1999) and Boering et al. (2004b) determined the global annual mean net isotope flux (NIF) from the stratosphere (ST) to the troposphere (T) for $\Delta^{'17}O$ of CO_2 using the $\Delta^{'17}O(CO_2)$-N_2O correlation as described in detail by Garofalo et al. (2019).

$$\Delta^{'17}O(CO_2) - NIF = MF \times [CO_2]_{ST} \times \left[m \times \frac{-L_{N_2O}}{MF} + \Delta^{'17}O(CO_2)_T \right] - MF \times [CO_2]_T \times \Delta^{'17}O(CO_2)_T \qquad (5)$$

The terms MF, L_{N_2O}, and m stand for the total air mass flux from the stratosphere to the troposphere, the global N_2O loss rate and the correlation slope between $\Delta^{'17}O$, respectively. In our analysis, this correlation slope is determined using a Williamson-York bivariate fit, accounting for uncertainties in both the $\Delta^{'17}O(CO_2)$ and N_2O data (Mikkonen et al., 2019). There is a significant variation in estimates for the air mass flux from the stratosphere to the troposphere. For instance, the estimates by Holton et al. (1995) and Appenzeller et al. (1996) differ by a factor of three in their calculated cross-tropopause air mass fluxes, but note that the troposphere definitions are also different. As described in Garofalo et al. (2019), the net isotope flux is not strongly sensitive to the actual air mass fluxes. Since the mole fraction of CO_2 in the lower stratosphere and troposphere is the same within about 1 %, equation 5 can be simplified to:

$$\Delta^{'17}O(CO_2) - NIF = -m \times L_{N_2O} \times [CO_2] \qquad (6)$$

The uncertainty in the estimated net annual mean flux of $\Delta^{'17}O(CO_2)$ depends on the uncertainty ~~in depends on the uncertainty~~ of m and L_{N_2O}. In our calculation, we used 370 ppm for $[CO_2]$, the average value for CARIBIC samples, most of them collected in the year 2001.

In the stratosphere the CO_2 and N_2O isotopes are influenced by different processes. N_2O is mainly destroyed by N_2O photolysis but its is also affected by $O(^1D)$ in the lower stratosphere and upper troposphere. Since N_2O photolysis and O_3

photolysis occur at different wavelengths, the relationship between $\Delta'^{17}O(CO_2)$ and N_2O contains valuable information about atmospheric chemistry and transport. The lifetime of N_2O varies with altitude. In the upper stratosphere and mesosphere, the N_2O lifetime decreases, leading to greater scatter. This scatter remains small until transport time becomes shorter than the N_2O lifetime. The scatter in $\Delta'^{17}O(CO_2)$ versus N_2O mixing ratio plots of $\Delta'^{17}O(CO_2)$ versus N_2O is mainly caused by latitudinal variations in the age of the air in the stratosphere. $\Delta'^{17}O(CO_2)$ values increase with altitude as N_2O mixing ratios decrease below ≈ 70 km. However, above 70 km, $\Delta'^{17}O(CO_2)$ begins to decrease with further decreases in N_2O mixing ratios. However, in the lower stratosphere and upper troposphere, where the lifetime of N_2O against photolysis is longer than the transport time, the scatter in N_2O values remains low (Liang et al., 2007a, 2008). The $\Delta'^{17}O(CO_2)$-N_2O correlation remains consistent both spatially and temporally in the lower stratosphere and the upper troposphere (Liang et al., 2007b, 2008). Since the net isotope flux of $\Delta'^{17}O(CO_2)$ is derived from samples from the lower stratosphere and upper troposphere, the observed variability (scatter) in the stratosphere does not affect the global average $\Delta'^{17}O(CO_2)$-N_2O slope used to estimate the flux of $\Delta'^{17}O(CO_2)$ from the stratosphere to the troposphere.

2.6 Estimating gross surface flux using $\Delta'^{17}O(CO_2)$

The CARIBIC samples analysed in this study cover latitudes from 30° south to 54° north (see Figure 1), we . We used these samples to estimate surface emissions using a mass balance box model calculation. The box model used in this study is not suitable to simulate for simulating the spatial and temporal variability of $\Delta'^{17}O(CO_2)$ (Koren et al., 2019). Our box model is an extended version of those used by Hoag et al. (2005) and Liang et al. (2017b), incorporating . Hoag et al. (2005) used a two-box model to explore the relative contributions to the production of $\Delta'^{17}O(CO_2)$ in the stratosphere, its flux to the troposphere and its destruction or dilution by various surface carbon fluxes in the troposphere. Liang et al. (2017b) used a one-box model, in which the major surface resetting processes were explicitly included to distinguish terrestrial fluxes from oceanic fluxes. In our model, we incorporated an intermediate upper troposphere (UT) box. AdditionallyFurthermore, our study includes measurements of $\Delta'^{17}O$ measurements from both hemispheres and different seasons. The $\Delta'^{17}O(CO_2)$ value in the UT depends on the $\Delta'^{17}O(CO_2)$ value of stratosphere (ST) and surface processes (assimilation/photosynthesis (A), respiration (R), soil invasion (SI), ocean (o) and anthropogenic emission (anth)) and the corresponding fluxes (F). At In steady state, the mass balance equation for $\Delta'^{17}O(CO_2)$ in the upper troposphere is:

$$
F_A \times \Delta_A \Delta'^{17}O + F_{anth} \times \Delta'^{17}O_{anth} + F_{ST} \times \left(\Delta'^{17}O_{ST} - \Delta'^{17}O_{UT} \right) + F_o \times \left(\Delta'^{17}O_o - \Delta'^{17}O_{UT} \right) +
$$
$$
F_R \times \left(\Delta'^{17}O_R - \Delta'^{17}O_{UT} \right) + F_{SI} \times \left(\Delta'^{17}O_{SI} - \Delta'^{17}O_{UT} \right) = 0 \tag{7}
$$

where $F_A = F_{al} - F_{la} = 0.88 \times GPP$ (Ciais et al., 1997a), with al, la, and GPP being atmosphere-to-leaf flux, leaf-to-atmosphere flux, and gross primary production, respectively. $\Delta_A\Delta'^{17}O$ is the discrimination against $\Delta'^{17}O$ during assimilation, and calculated as $\Delta_A\Delta'^{17}O = (\Delta'^{17}O_{UT} - \Delta'^{17}O_M) \times (-0.150 \times e^{3.707 \times \frac{c_m}{c_a}} + 0.028)$ as described by Adnew et al. (2020a) Adnew et al. (2020b) (see the supplementary material for more detail). This parameterization was derived from leaf cuvette studies using both C_3 and C_4 plants under different light conditions. c_m and c_a represent the CO_2 mole fraction in the meso-

phyll and the atmosphere, respectively. $\Delta^{'17}O_M$ is the $\Delta^{'17}O$ of CO_2 in the mesophyll, calculated from the $\Delta^{'17}O$ value of meteoric water (MW) (Landais et al., 2007; Barkan and Luz, 2012; Bottinga and Craig, 1968; Brenninkmeijer et al., 1983), see also the supplementary material.

225   The estimates of soil invasion fluxes are highly uncertain, the reported values in the literature vary from < 10 PgC/yr (Stern et al., 2001) to 450 PgC/yr (Wingate et al., 2009). For this study, we assume that F_{SI} and F_R are equal, and $F_A = 0.88 \times GPP = 0.88 \times (NEP - F_R)$ (Liang et al., 2017b). Substituting this term in equation 7:

$$F_A \times \Delta_A \Delta^{'17}O + F_{anth} \times \Delta^{'17}O_{anth} + F_{ST} \times \left(\Delta^{'17}O_{ST} - \Delta^{'17}O_{UT} \right) + F_o \times \left(\Delta^{'17}O_o - \Delta^{'17}O_{UT} \right) +$$
$$\left(\frac{F_A}{0.88} - NEP \right) \times \left(\Delta^{'17}O_R - \Delta^{'17}O_{UT} \right) + \left(\frac{F_A}{0.88} - NEP \right) \times \left(\Delta^{'17}O_{SI} - \Delta^{'17}O_{UT} \right) = 0 \qquad (8)$$

The $\Delta^{'17}O_{anth}$ value is -0.446 ± 0.077 ‰ (Horváth et al., 2012; Laskar et al., 2016). The $\Delta^{'17}O_o$ value is calculated from
230   the $\Delta^{'17}O$ value of ocean water (OW) (Table 1). Similarly, the $\Delta^{'17}O$ values for soil invasion and respiration are derived from the $\Delta^{'17}O$ value of meteoric water (Liang et al., 2023; Koren et al., 2019; Hofmann et al., 2017). For the calculations, we used a surface temperature of 15°C, and a relative humidity of 75 % (Dai, 2006). The sensitivity of $\Delta_A \Delta^{'17}O$ to temperature and relative humidity is shown in Figure S1 of the supplementary material. The value of $\Delta_A \Delta^{'17}O$ increases with an increase in relative humidity but decreases with increasing temperature. Using the parameters described above and provided in Table
235   1 and Equation 8, we estimated the gross primary production (GPP), surface flux (including land and ocean) and the oxygen isotope residence time (turnover time) of CO_2 in the atmosphere. The oxygen isotope residence time of CO_2 in the atmosphere is defined by the ratio of the atmospheric CO_2 mass loading (M_a) and the CO_2 surface flux (Welp et al., 2011). The error for all estimated values is determined using a Monte Carlo simulation ~~using~~ with 10^6 runs, where values of the input ~~parameter~~ parameters are randomly picked from ~~an input value distribution of these parameters~~ a normal distribution defined by their
240   uncertainty.

The sensitivity of GPP to relative humidity, temperature, the $\Delta^{'17}O$ value of the upper troposphere, and the net flux of $\Delta^{'17}O$ from the stratosphere to the troposphere is shown in Figures S2 and S3 of the supplementary material. A higher net flux of $\Delta^{'17}O$ to the troposphere leads to an increase in GPP to fulfill the isotope balance of equation 8. An increase in relative humidity leads to a decrease in GPP due to an increase in $\Delta_A \Delta^{'17}O$. Conversely, an increase in temperature results in an
245   increase in GPP, as higher temperatures cause a decrease in $\Delta_A \Delta^{'17}O$, as described above. The parameters used in the mass balance calculations and their errors are provided in Table 1.

2.7 De-trending and classification of samples into upper troposphere and stratosphere

~~For comparison with~~ To ensure comparability of previously published data and ~~between~~ the CARIBIC and StratoClim samples measured in this study, all N_2O measurements were trend-corrected to the year 2001 following a similar approach described in
250   Koren et al. (2019).

$$N_2O_{det} = N_2O_{obs} \times \left[1 - \frac{N_2O_{growthrate}}{N_2O_{ref}} \times (t_{ref} - t_{obs}) \right]^{-1} \qquad (9)$$

Table 1. Summary of parameters used for the box model mass balance calculation in Equation 8. T and RH represents temperature in Kelvin and relative humidity near the Earth's surface, respectively.

Parameter	value or description	ref
α_{trans}^{18}	$1.002644 - \frac{3.206}{T} + \frac{1534}{T^2}$	Bottinga and Craig (1968)
$\alpha_{CO_2-H_2O}^{18}$	$\frac{17.604}{T} + 0.98207$	Brenninkmeijer et al. (1983)
$\alpha_{diff-water}^{18}$	$1.0016\,‰$	Farquhar and Lloyd (1993)
$\alpha_{diff-soil}^{18}$	$1.0072\,‰$	Miller et al. (1999)
θ_{trans}	$0.522 - 0.008 \times RH$	Landais et al. (2007)
$\theta_{CO_2-H_2O}$	0.5229	Barkan and Luz (2012)
θ_{diff-H_2O}	0.50	calculated
$\theta_{diff-air}$	0.509	Young et al. (2002)
GPP	Gross primary production	calculated
F_A	$0.88 \times$ GPP	Ciais et al. (1997b)
F_{al}	$\frac{c_a}{c_a-c_m} \times F_A$	Farquhar et al. (1993)
F_{la}	$\frac{c_m}{c_a-c_m} \times F_A$	Farquhar et al. (1993)
$\frac{c_m}{c_a}$	0.65	Farquhar et al. (1993)
M_a	807 ± 6 PgC	Stocker et al. (2013)
F_o	80 ± 6 PgC/yr	Stocker et al. (2013)
F_{anth}	9 ± 0.8 PgC/yr	Stocker et al. (2013)
NEP	10 PgC/yr	Saugier et al. (2001)
$\Delta'^{17}O_{MW}$	$0.033 \pm 0.005\,‰$	Barkan and Luz (2012)
$\theta_{deg-equ}$	1.0	assumed
$\Delta'^{17}O_{OW}$	$-0.005 \pm 0.001\,‰$	Barkan and Luz (2012)

Here, N_2O_{obs}, N_2O_{det}, N_2O_{ref} and $N_2O_{growthrate}$ refer to the observed and detrended mole fractions of N_2O, the mole fraction of N_2O at the reference time and the growth rate of N_2O in the troposphere, respectively. The variables t_{obs} and t_{ref} represent the time of observation and the reference time (1 July 2001). The growth rate of N_2O in the troposphere, used in this study, is 0.75 ppb/year (Stocker et al., 2013). The mole fraction of N_2O at the reference time (1 July 2001) is 316.24 ppb (Lan et al., 2024).

The mole fraction of CH_4 in the StratoClim data was detrended to 2007 using an average growth rate of 12 ppb/year (Nisbet et al., 2019). The 2007 mole fraction of CH_4 is assumed to be the same as the CH_4 mole fraction in 2001, since the atmospheric CH_4 mole fraction was stable between 2000 and 2007 (Nisbet et al., 2019).

We used the N_2O-CO correlation to classify air samples into upper troposphere and stratospheric samples as described in detail by Assonov et al. (2013). The N_2O maintains a nearly constant tropospheric concentration, as it is minimally affected by chemical processes and has no significant atmospheric sources. This stability allows stratospheric influence to be more

easily identified. The correlation between N_2O and CO forms an L-shaped curve, similar to O_3-CO correlations observed during stratosphere-to-troposphere air mass mixing events (Assonov et al., 2013). As a result, the troposphere corresponds to the horizontal branch (high N_2O, variable CO), while the stratosphere, free from tropospheric influence, corresponds to the vertical branch (low CO, variable N_2O). The CARIBIC samples are mostly from the upper troposphere (UT) and include a few from the lower stratosphere (see Figure S4 in the supplementary material). Based on the mole fraction of N_2O, we grouped the $\Delta'^{17}O$ values into two categories: upper troposphere (UT) samples ($N_2O \geq 313.5$ ppb) and the lower stratosphere (LS) samples ($N_2O < 313.5$ ppb). We further divided the lower stratosphere into two subgroups: $313.5 > N_2O > 306$ ppb and $N_2O < 306$ ppb. Furthermore, we used a zonal average tropopause pressure simulated using the TM5 model as outlined in Krol et al. (2018), and the *age of air* tracer, to support the classification of samples into upper tropospheric and stratospheric. The age of air was calculated using SF_6 measurements as described in Krol et al. (2018). Most of the samples classified as upper tropospheric based on the mole fraction of N_2O were collected far below the tropopause whereas the samples classified as stratospheric were collected above or close to the tropopause with a few exceptions (see Figure S5 in the supplementary material).

2.8 Sampling

Air samples were collected from the upper troposphere and stratosphere during two different international projects, CARIBIC and StratoClim, which are shortly described below. Figure 1 shows the geographical coordinates of the sampling locations for the samples measured in this study.

2.7.1 CARIBIC samples

In the CARIBIC project (Civil Aircraft for the Regular Investigation of the atmosphere Based on an Instrument Container, CARIBIC,), samples were collected using a Boeing 767 aircraft (LTU, Germany). The flights operated at typical commercial cruising altitude between 9 and 12 km, i.e., which is the upper troposphere-lower stratosphere region at higher latitudes and the upper troposphere region in the mid latitudes and tropics (Assonov et al., 2010). The details of the CARIBIC instrument container are described in Brenninkmeijer et al. (1999). The payload of the flights before 2003 included large stainless steel canisters for collecting whole air samples (WAS) (sample size ≈ 340 L STP) at several locations along the flight path. On a single flight 12 discrete samples were collected. Each sample collection took about 20 min which corresponds to a horizontal distance of 250 km (Brenninkmeijer et al., 1999). The samples collected are relatively dry since the ambient temperature was always below –30 °C and the relative humidity was about 0.44 % at 20 °C (Assonov et al., 2009b). The air samples were processed soon after they returned to the Division of Atmospheric Chemistry, Max Planck Institute for Chemistry, Mainz, Germany (Pupek et al., 2005). The processing included the extraction of CO_2 and CO for isotope analysis, including radiocarbon (Brenninkmeijer, 1993; Assonov et al., 2009b) as well as measurement of several other trace gases including , and (Brenninkmeijer et al., 1999). The CARIBIC container was also equipped with an automated in-situ analyzer for (UV absorption), CO (gas chromatography (GC)) and other parameters (Brenninkmeijer et al., 1999). In this study we measured the $\Delta'^{17}O$ value of 50 CARIBIC samples.

2.7.1 ~~StratoClim samples~~

~~35 additional air samples were collected on the high-altitude M55 Geophysica aircraft during two campaigns of the StratoClim project () (Stefanutti et al., 1999; Cairo et al., 2010) in 2016 and 2017. In 2016, three flights were conducted over the Mediterranean region from Kalamata, Greece ($37°2'$N and $22°7'$E) between August 30 and 6 September and eight flights were conducted in 2017 over the Indian subcontinent from Kathmandu, Nepal ($27°46'$N and $85°16'$E) between 27 July and 10 August. The whole air sampler of the Institute for Marine and Atmospheric research Utrecht (IMAU), Utrecht University was used to compress air into 2 L pre-evacuated stainless-steel canisters (Kaiser et al., 2006). We analysed 16 samples from the 2016 flights and 19 samples from the 2017 flights (Table S3). Further details on sample collection using the Geophysica aircraft can be found in Kaiser et al. (2006) and Stefanutti et al. (1999).~~

~~Geographical location of the CARIBIC (black markers), StratoClim2016 (blue circles) and StratoClim2017 (blue stars) air samples measured in this study. Upper tropospheric CARIBIC samples are categorized based on the geographical location where they are collected. These categories include Southern Hemisphere samples, Northern Hemisphere samples, African samples (longitude between $7°$ and $45°$), Asian samples (longitude $> 45°$), and American samples (longitude $< 0°$).~~

2.8 ~~Extraction of~~

~~For the StratoClim samples, the was extracted from the whole air samples using a cryogenic extraction system developed at Utrecht University (Adnew et al., 2020a, 2023). The extraction system was made of electropolished stainless steel and has four traps. The first two traps remove moisture and condensable organics at dry ice temperature whereas the third and fourths traps were used to collect at liquid nitrogen temperature. The extraction was performed at a flowrate of 55 mL/min.~~

~~For the CARIBIC samples, the had previously been extracted at the Max Planck Institute for Chemistry, Mainz, as described in Assonov et al. (2009b) and Pupek et al. (2005). Two "Russian Doll" cryogenic traps (Brenninkmeijer and Röckmann, 1996; Brenninkmeijer immersed in liquid nitrogen trapped all condensable gases including , , and most organics. After pumping out non-condesables, the traps were slowly heated and the evolving and was trapped in a U-trap cooled with liquid nitrogen while the remained trapped in the Russian Doll Traps. The collected was further dried using and flame-sealed in clean vials made of borosolicate glass (Assonov et al., 2009b; Pupek et al., 2005).~~

2.8 ~~Measurement of δ^{13}C, δ^{18}O and Δ'^{17}O of~~

~~The δ^{18}O and δ^{13}C values presented below were measured using a Delta^{PLUS} V isotope ratio mass spectrometer (ThermoScientific, Germany) in dual inlet mode at Utrecht University. The interference of was corrected using: $\delta^{18}O = \delta^{18}O_{Measured} + \frac{[N_2O]}{[CO_2]}\left(\frac{347}{1000}\right)$ and $\delta^{13}C = \delta^{13}C_{Measured} + \frac{[N_2O]}{[CO_2]}\left(\frac{250}{1000}\right)$ (Friedli and Siegenthaler, 1988; Sirignano et al., 2004). Figure 2 shows a comparison of the the δ^{18}O and δ^{13}C of of CARIBIC samples measured in this study with those previously measured at the Max-Planck-Institute for Chemistry and reported in Assonov et al. (2009b, a, 2010).~~

~~The δ^{18}O and δ^{13}C of CARIBIC samples and comparison with values published in Assonov et al. (2009b, a, 2010).~~

The $\delta^{18}O$ values measured in this study are systematically higher compared to the measurement by Assonov et al. (2010) by $0.096 \pm 0.008\,\permil$. For $\delta^{13}C$ values, our measurement is also higher by $0.089 \pm 0.011\,\permil$. The reported error is the 95 % confidence limit (standard error of the mean multiplied by Student's t-factor). The tight distribution of differences is of the order of the measurement precision, which suggests that the isotopic composition of the samples remained stable during long-term storage in borosilicate glass vials and that the mean offset is due to scale differences. These observed offsets are consistent with the scale uncertainty reported by Assonov et al. (2009a) and better than typical inter-laboratory uncertainties (Levin et al., 2007).

The $\Delta'^{17}O$ of the was determined using the -exchange method (Adnew et al., 2019, 2022, 2023; Barkan et al., 2015) at Utrecht University. Equal amounts of sample and the laboratory reference (with known isotopic composition) were allowed to exchange isotopes for 2 hours in a quartz reactor at 750°C in the presence of platinum sponge at the bottom of the reactor. After the reaction, the mixture was passed through a liquid nitrogen-cooled trap to condense the and the was collected in a separate trap on 3 pellets of 5Åmolecular sieve (1.6mm, Sigma-Aldrich, USA) at liquid nitrogen temperature. The was then transferred to the bellows of the dual inlet system of a Delta^{PLUS} V isotope ratio mass spectrometer (ThermoFisher Scientific, Germany) and measured for its isotope composition. The $\Delta'^{17}O$ value of the original was calculated from the change in the isotopic composition of the non-reacted and reacted , and knowledge of the precise steady-state -isotope fractionations (Adnew et al., 2019; Barkan et al., 2015). The precision of the isotope measurements was $0.007\,\permil$, $0.03\,\permil$ and $0.008\,\permil$ for $\delta^{13}C$, $\delta^{18}O$ and $\Delta'^{17}O$ respectively (Adnew et al., 2019, 2020a, 2023).

3 Results

Figure 3a shows $\Delta'^{17}O(CO_2)$ as a function of latitude for the CARIBIC samples. The samples classified as upper tropospheric, $\Delta'^{17}O(CO_2)$ do not show geographic variations between large regions referred to as America, Asia and Africa, respectively (see Figure 1) and no statistically significant difference in $\Delta'^{17}O(CO_2)$ between the hemispheres (see Figure 3b). Table S2 in the supplementary material presents the mole fraction of CO_2, O_3, CO, N_2O and CH_4, along with the isotopic composition of CO_2 ($\delta^{13}C$, $\delta^{18}O$ and $\Delta'^{17}O$) for the analyzed CARIBIC samples. Similarly, the mole fraction of CO_2 and other trace gases (O_3, CO, N_2O and CH_4), along with the isotopic composition of CO_2 for StratoClim samples is shown in Table S3 of the supplementary material.

Figure 4 shows the correlation of $\Delta'^{17}O(CHCO_2)$ measurements with the mole fractions of CH_4 and N_2O. For both sets of samples (CARIBIC and StratoClim), N_2O and $\Delta'^{17}O(CO_2)$ are clearly correlated with R^2 values of ≥ 0.9 as shown in Figure 4. Similar tight correlations between N_2O and $\Delta'^{17}O(CO_2)$ were reported in the previous studies as shown in Figure 6. Interestingly, StratoClim samples plot in two distinct groups of N_2O-$\Delta'^{17}O(CO_2)$ correlations. Most of the StratoClim samples with $\Delta'^{17}O < 0.2\,\permil$ have a similar N_2O-$\Delta'^{17}O$ slope as the CARIBIC samples as shown in Figure 4a. However, unexpectedly the N_2O-$\Delta'^{17}O$ correlation slope for most of StratoClim samples with $\Delta'^{17}O > 0.2\,\permil$ is much lower ($-0.017\,\permil$ per ppb) (see Figure 4a).
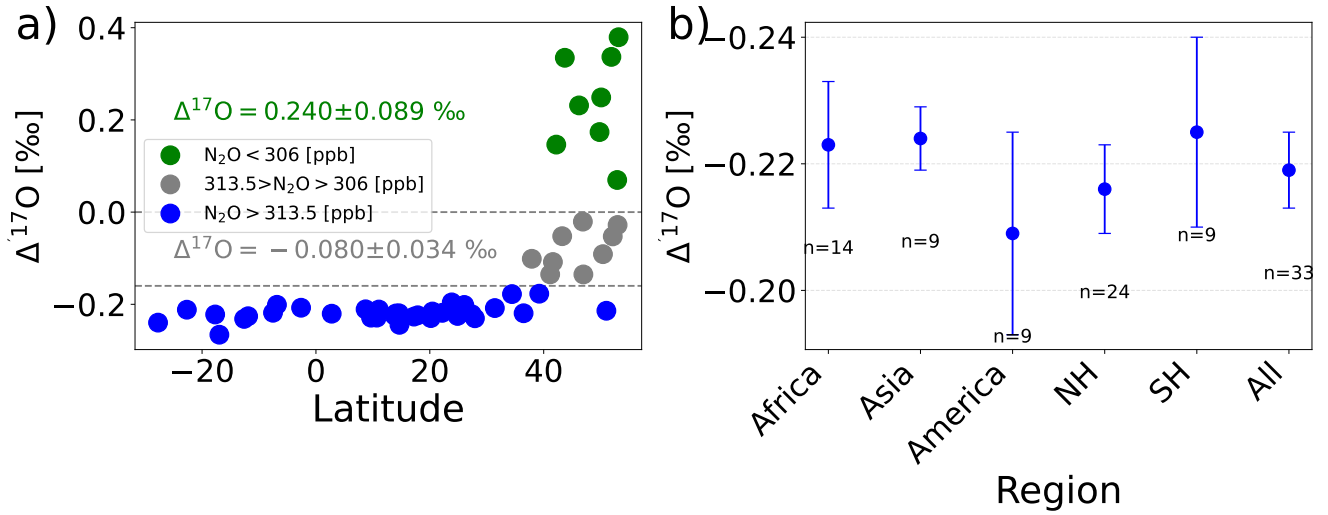
Figure 3. a) $\Delta'^{17}O(CO_2)$ values of CARIBIC samples as a function of latitude. The $\Delta'^{17}O$ values are grouped into three categories based on the mole fraction of N_2O as described in the text. b) average $\Delta'^{17}O$ value of all upper tropospheric CARIBIC air samples and larger geographical regions. The errors are the standard error of the mean multiplied by the student t-factor for the 95 % confidence limit. *n, SH* and *NH* stands for the number of samples, Southern Hemisphere and Northern Hemisphere, respectively.

As shown in Figure 4b, there is a strong inverse correlation between CH_4 and $\Delta'^{17}O$. For the StratoClim samples, the correlation is higher compared to the CARIBIC samples, with R^2 values of ≥ 0.9 and 0.79, respectively. For both CARIBIC and StratoClim samples with $\Delta'^{17}O < -0.2$ ‰ , no clear correlation between CH_4 and $\Delta'^{17}O$ can be established (see Figure 4b).

~~a) Three isotope plot for StratoClim (stars) and CARIBIC (open circles) samples. The linear-regression is a fit to the samples identified as upper tropospheric based on the N_2O mole fraction. The color bar indicates the age of the air mass for the StratoClim samples reported in Adcock et al. (2021). The stated errors for the linear regression parameters are the 95 % confidence intervals. b) Relationship between the age of the air and $\Delta'^{17}O(CO_2)$ for StratoClim samples. The data points marked in red indicate samples with a low -$\Delta^{17}O$ correlation slope.~~

Figure 5 shows the three-isotope plot for both CARIBIC and StratoClim samples. The three-isotope plot of upper-tropospheric samples shows a tight correlation for both CARIBIC and StratoClim samples with slopes of 0.540 ± 0.005 and 0.556 ± 0.012, respectively (Figure 5). For the StratoClim samples with higher stratospheric influence the $ln(\delta^{17}O+1)$ vs $ln(\delta^{18}O+1)$ is poorly correlated. It is apparent in Figure 5a that the vertical offsets from the fit line defined by the upper tropospheric samples get larger for larger stratospheric age, which is shown as colour coding. Figure 5b shows the correlation between the age of the air and $\Delta'^{17}O(CO_2)$. An increase in the age of the air correlates well with a progressive enrichment of $\Delta'^{17}O(CO_2)$.

Figure 6 shows a comparison of our CARIBIC and StratoClim samples measured in this study with previously published $\Delta'^{17}O$ measurements of upper-tropospheric and stratospheric CO_2 (Thiemens et al., 1995a, c; Alexander et al., 2001; Läm-
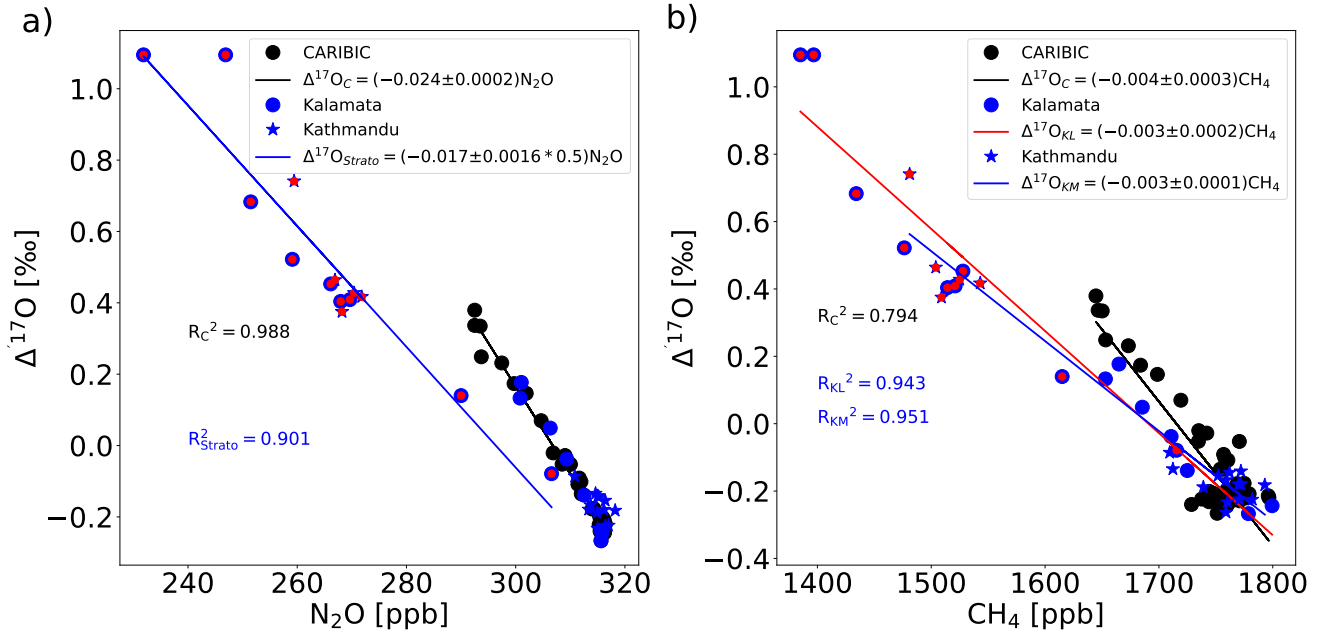
**Figure 4.** Correlation of $\Delta'^{17}O(CO_2)$ with a) N_2O for StratoClim samples (StratoClim-2016 is Kathmandu (KT, blue stars) and StratoClim-2017 is Kalamata (KL, blue circles)) and CARIBIC samples (black circles) and b) CH_4. The errors of the linear regression slopes are the 95 % confidence interval. The data points marked in red indicate StratoClim samples with a low N_2O-$\Delta^{17}O$ correlation slope.

merzahl et al., 2002; Boering et al., 2004b; Wiegel et al., 2013; Kawagucci et al., 2005; Yeung et al., 2009). Four different characteristics are shown: The three-isotope plot (Figure 6a), $\Delta'^{17}O$ as a function of altitude (only for StratoClim samples) (Figure 6b), the N_2O-$\Delta'^{17}O$ correlation (Figure 6c) and the CH_4-$\Delta'^{17}O$ correlation (Figure 6d). In these overview plots of N_2O-$\Delta'^{17}O$ and CH_4-$\Delta'^{17}O$ plots, the new CARIBIC and StratoClim measurements are almost indistinguishable from the

380 measurements reported in the literature. However, when we zoom in and compare the correlation slopes, clear differences for some of the measurements become apparent such as shown in Figure 4a for the variation in the N_2O-$\Delta'^{17}O$ correlation between CARIBIC and StratoClim samples.

~~Figure 5 shows the three-isotope plot for both CARIBIC and StratoClim samples. The three-isotope plot of upper-tropospheric samples shows a tight correlation for both CARIBIC and StratoClim samples with slopes of 0.540 ± 0.005 and 0.556 ± 0.012,~~

385 ~~respectively (Figure 5). For the StratoClim samples with higher stratospheric influence the $ln(\delta^{17}O + 1)$ vs $ln(\delta^{18}O + 1)$ is poorly correlated. It is apparent in Figure 5a that the vertical offsets from the fit line defined by the upper tropospheric samples get larger for larger stratospheric age, which is shown as colour coding. Figure 5b shows the correlation between the age of the air and $\Delta'^{17}O(CO_2)$. An increase in the age of the air correlates well with a progressive enrichment of $\Delta'^{17}O(CO_2)$.~~

16
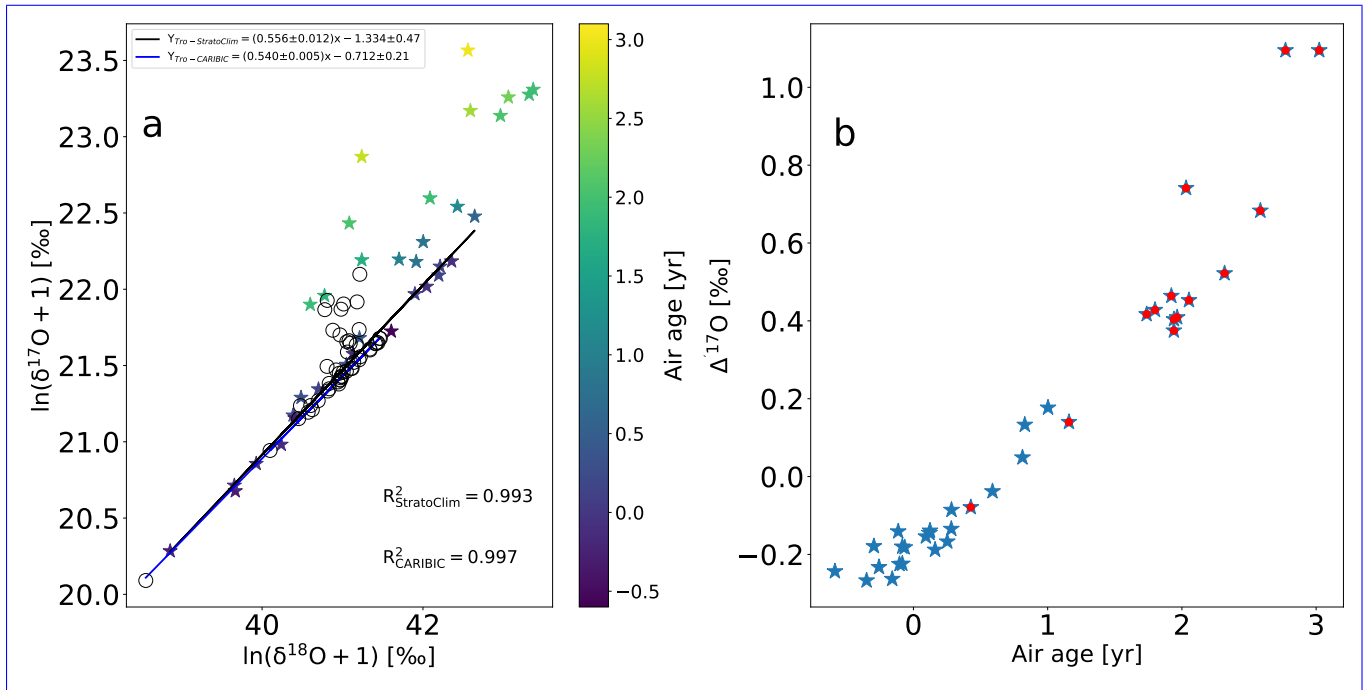
Figure 5. a) Three isotope plot for StratoClim (stars) and CARIBIC (open circles) samples. The linear-regression is a fit to the samples identified as upper tropospheric based on the N_2O mole fraction. The color bar indicates the age of the air mass for the StratoClim samples reported in Adcock et al. (2021). The stated errors for the linear regression parameters are the 95 % confidence intervals. b) Relationship between the age of the air and $\Delta'^{17}O(CO_2)$ for StratoClim samples. The data points marked in red indicate samples with a low N_2O-$\Delta^{17}O$ correlation slope.

4 Discussion

390   When the CARIBIC and StratoClim samples presented here are separated into upper tropospheric and stratospheric based on N_2O levels, these two groups exhibit distinct characteristics. The upper tropospheric samples show a tight correlation on the three-isotope plot, whereas the stratospheric samples display significant variability without a clear correlation. Interestingly, the three-isotope slopes (from a linear fit to the data) for the upper tropospheric samples are higher than the expected canonical range for tropospheric samples ($\lambda > 0.5309$). This indicates that upper tropospheric air already has a stratospheric influence.

395   The contribution of stratospheric air in the CARIBIC samples is evident from an excellent correlation between $\Delta'^{17}O(CO_2)$ and both $^{14}C(CO)$ and O_3, as illustrated in Figure 7. Both ^{14}CO and O_3 are reliable tracers for stratospheric air (Brenninkmeijer et al., 1995). Similar correlations between ^{14}CO and $\Delta'^{17}O(CO_2)$ have been previously reported for stratospheric CO_2 (Thiemens et al., 1995c; Brenninkmeijer et al., 1995).

The observed scatter in the three-isotope plot for the stratospheric samples is conceptually similar to the scatter reported in
400   previous studies (Boering et al., 2004b; Wiegel et al., 2013; Mrozek et al., 2017; Thiemens et al., 1995a). In these publications
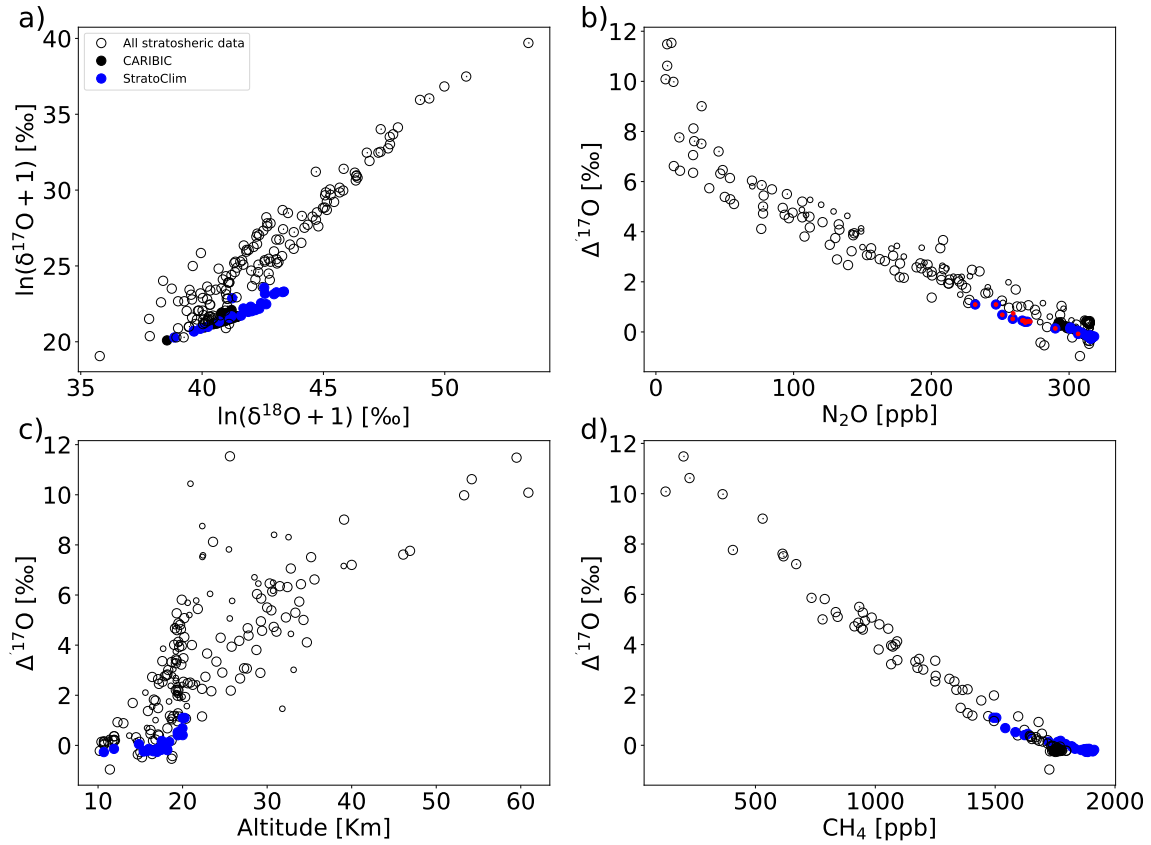
Figure 6. Comparison of results from CARIBIC samples (black circles) and StratoClim samples (blue circles) to previous publications (open circles). a) three isotope plot, b) correlation of $\Delta'^{17}O(CO_2)$ with N_2O. The data points marked in red indicate StratoClim samples with a low N_2O-$\Delta^{17}O$ correlation slope. c) correlation of $\Delta'^{17}O(CO_2)$ with altitude and d) correlation of $\Delta'^{17}O(CO_2)$ with CH_4. Previous stratospheric samples are from (Thiemens et al., 1995a, c; Alexander et al., 2001; Lämmerzahl et al., 2002; Boering et al., 2004b; Wiegel et al., 2013; Kawagucci et al., 2005; Yeung et al., 2009)

it was mostly assumed to be due to the low precision of the measurement method. However, in this study, with high precision measurements, a similar scatter in the three-isotope plot is observed, demonstrating that the scatter observed in the three-isotope plot for stratospheric samples is a real signal of mixing, transport and production of $\Delta'^{17}O(CO_2)$ (i.e. exchange between $O(^1D)$ and CO_2). The tight correlation with the age of air provides a clear clue to explain this lack of correlation. The longer CO_2
405   has been exposed to the stratospheric CO_2-$O(^1D)$ exchange, the higher the $\Delta'^{17}O(CO_2)$ signal is (Yung et al., 1997a; Gamo et al., 1995; Yung et al., 1991a). The fact that the different samples do not line up on a single three isotope correlation line

18

shows that we have sampled stratospheric air originating from different upper tropospheric "entry values" before entering the stratosphere. These differences in entry values are likely driven by the seasonality of $\delta^{17}O(CO_2)$ and $\delta^{18}O(CO_2)$. Thus, different tropospheric air masses have entered the stratosphere from various points along the correlation line established by the upper tropospheric samples. Once in the stratosphere, photochemical isotope exchange with O^1D occurs, and the samples progressively acquire a higher $\Delta'^{17}O(CO_2)$ signature as the sampled air resided longer in the stratosphere. This is clearly demonstrated by the strong correlation between $\Delta'^{17}O(CO_2)$ and the age of air, and it was not clearly visible in previous studies because of the higher measurement uncertainty.

Interestingly, despite our high measurement precision, we did not observe significant geographic variations in $\Delta'^{17}O(CO_2)$ of CARIBIC air samples classified as upper troposphere (see Figure 3b), which could potentially arise from varying stratospheric and tropospheric air mass influences in different geographical regions. The lack of geographic variability contrasts with the reported regional $\Delta'^{17}O(CO_2)$ variability at the surface (Liang et al., 2017a, 2023). Apparently, the variability at the surface, caused by sources and sinks of CO_2, including isotope exchange with surface water reservoirs and anthropogenic emissions, is no longer visible in the upper troposphere, where the reservoir seems to be relatively well mixed in terms of $\Delta'^{17}O(CO_2)$. Air masses in the upper troposphere experience rapid horizontal mixing, which can explain the uniform stratospheric influence in the CARIBIC samples.
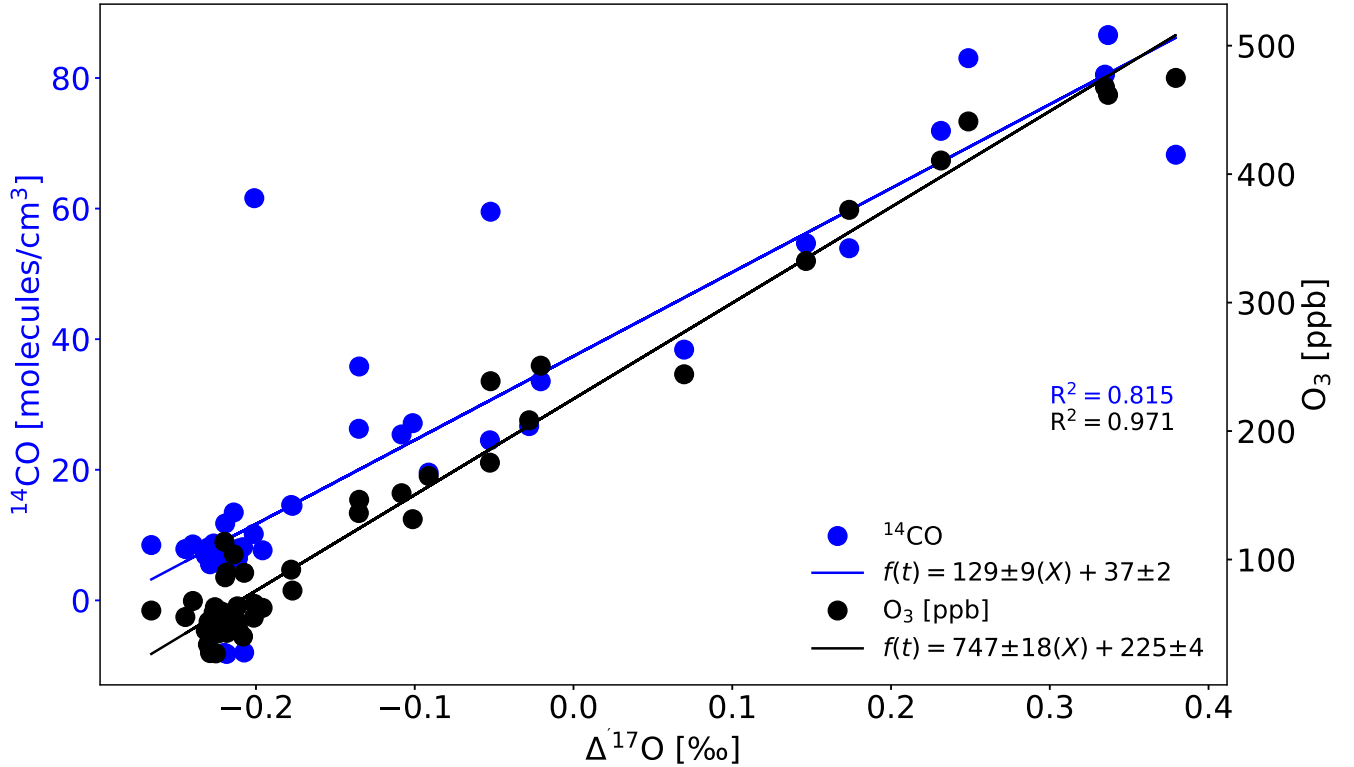
Figure 7. Correlation of $\Delta'^{17}O$ with stratospheric air tracers ^{14}CO and O_3 for CARIBIC samples.
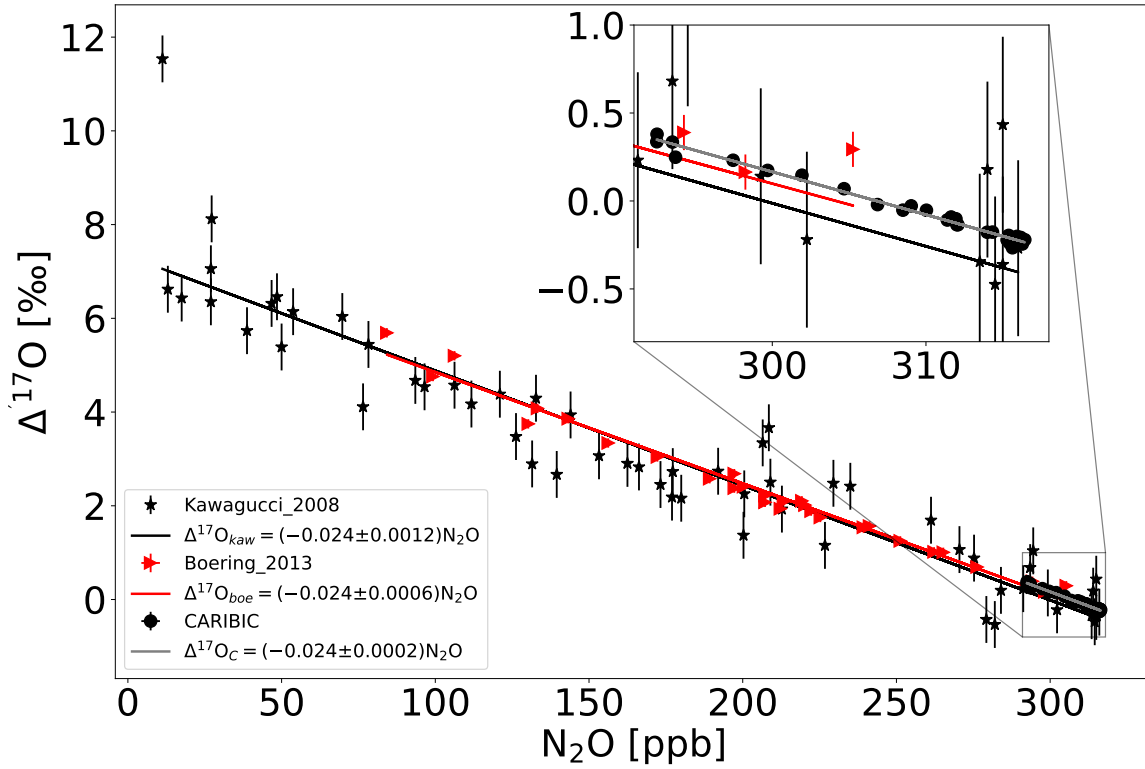
Figure 8. $\Delta'^{17}O - N_2O$ correlation for CARIBIC samples and measurements of Kawagucci et al. (2008) and Boering et al. (2004b). The inset shows the zoom to the data close to the tropopause. For the CARIBIC samples measured in this study, the error-bars are smaller than the data markers. For the linear regression slopes, the errors are the 95 % confidence interval.

The slope of two tracers near the tropopause is a measure of their relative net fluxes between troposphere and stratosphere (Plumb and Ko, 1992; Plumb, 2007). The slope of $N_2O-\Delta'^{17}O(CO_2)$ was first used by Luz et al. (1999) and Boering et al. (2004b) to quantify the so-called isoflux of $\Delta'^{17}O(CO_2)$ from the stratospheric into the troposphere. Previous measurements had a lower precision and could not define the slope close to the tropopause, but only for older stratospheric air. Our high precision measurements of $\Delta'^{17}O(CO_2)$ allow to determine the $N_2O-\Delta'^{17}O(CO_2)$ slope right down to the tropopause. Figure 8 shows that the slope for CARIBIC samples is indistinguishable from the correlations reported in the previous studies for stratospheric samples (-0.024 ‰/ppb) (Kawagucci et al., 2008; Wiegel et al., 2013; Boering et al., 2004b). However, the regression lines have an offset. This offset likely arises from variations in the $\Delta'^{17}O(CO_2)$ measurement scales among different laboratories. Recently, Liang et al. (2023) reported a scale offset in $\Delta'^{17}O(CO_2)$ of 0.037 to 0.042 ‰ between two laboratories (Institute of Earth Sciences, Academia Sinica and Institute of Earth Sciences, Hebrew University of Jerusalem). To optimize

the application of $\Delta'^{17}O(CO_2)$ measurements, the implementation of interlaboratory calibration is crucial (Adnew and Röck-mann, 2022). A recent study by Laskar et al. (2019) reported a higher slope (0.036 ‰/ppb) for the N_2O-$\Delta'^{17}O$ correlation of CARIBIC samples collected during two flights. The samples they analyzed ~~are~~ mostly represent upper troposphere air, evident

435 from a lower O_3 mole fraction compared to the CARIBIC samples measured in this study. This is supported by the relatively low three-isotope slope of 0.48 reported by Laskar et al. (2019) compared to the samples measured in this study (> 0.54). Furthermore, their samples cover only a very small range of N_2O (only 3.5 ppb difference, i.e. between 311.5 and 315 ppb) which likely leads to a high error in the determination of the N_2O-$\Delta'^{17}O(CO_2)$ correlation slope.

In contrast, for the StratoClim samples, the N_2O-$\Delta'^{17}O(CO_2)$ correlation shows an unexpectedly low slope of -0.017

440 ‰/ppb, which is about 1.5 times lower than for the CARIBIC and other stratospheric samples (Figure 4). All our samples were measured in the same laboratory and on the same analytical system. We suggest that the lower N_2O-$\Delta'^{17}O$ correlation slope for StratoClim samples is due to enhanced vertical mixing during the Asian summer monsoon anticyclone (ASMA), as these samples were collected during mid-June to early September. The ASMA causes deep convection and anticyclonic flow in the upper troposphere and lower stratosphere (UTLS) where tropospheric air masses are uplifted into the UTLS (Park et al., 2009;

445 Vogel et al., 2015, 2016; Brunamonti et al., 2018). The lifetime for CO_2 isotopic exchange is much slower than the transport time at all altitudes, whereas the photochemical production and quenching rates for $O^1(D)$ are much faster than transport processes. Therefore, the isotopic composition of stratospheric CO_2 should reflect both the variety of transport histories of air parcels and the sources of $O^1(D)$ (Liang et al., 2007b; Boering et al., 2004b). Furthermore, throughout the entire atmosphere, the CO_2 isotopic exchange time is longer than the transport time. However, the lifetime of N_2O varies with altitude. In the lower

450 stratosphere, the lifetime of N_2O against photolysis is longer than the transport time, resulting in less variability in the region. ~~However~~In contrast, in the middle ~~and~~ stratosphere the N_2O life time decreases resulting a different N_2O-$\Delta'^{17}O$ correlation slope (Liang et al., 2008). The influence of vertical mixing on N_2O-$\Delta'^{17}O$ correlations was investigated in a model study by Liang et al. (2007b). Indeed, they found that an increase in the vertical eddy diffusion coefficient - thus more vigorous vertical mixing - leads to a lower slope of the N_2O-$\Delta'^{17}O$ correlation. This supports our hypothesis that the low correlation for the

455 StratoClim samples is caused by intense vertical mixing in the ASMA. An independent indication for the enhanced mixing is the scatter observed in three isotope plot and air age variability for the samples classified as stratospheric (Figure 5). Enhanced mixing, probably caused by deep convection and anticyclone flow in the upper troposphere and lower stratosphere, is consistent with the enhanced mole fraction of ozone-depleting substances in the samples collected in the same flight (Adcock et al., 2021).

High-precision N_2O-$\Delta'^{17}O(CO_2)$ correlation can thus help identify enhanced mixing of tropospheric air into the strato-

460 sphere and maybe a measurable tracer to quantify the intensity of eddy diffusion/transport (Liang et al., 2007b; Boering et al., 2004b). There are many other indicators for enhanced mixing above the tropopause due to ASMA including a 25 % increase in long-lived ozone-depleting substances in the upper troposphere-lower stratosphere from the same samples (Adcock et al., 2021) and a contribution of about 30 % of young tropospheric air in the extratropical lower stratosphere in the Northern Hemi-sphere due to ASMA (Vogel et al., 2016). Recently, Ma et al. (2022) reported that 30 % to 50 % of the air mass in the UTLS

465 above the ASMA region is mixed, with the highest mixing occurring around 16.5 km altitude. Moreover, for StratoClim sam-ples collected over the Indian subcontinent in Kathmandu (2017) in the tropopause region, the three major chlorinated very

short-lived substances were enhanced up to 136 % compared to typical tropical tropopause values in 2013–2014. In contrast, only a 10 % increase was observed in ground-based measurements from 2014 to 2017 (Adcock et al., 2021; Engel et al., 2019).

For the StratoClim samples, the CO mole fraction reached a stratospheric background value at a potential temperature of 420 K, and the N_2O mole fraction remained similar to the tropospheric value up to 400 K, as described in detail by von Hobe et al. (2021) and Vogel et al. (2024). The deviation of the correlation between N_2O and $\Delta'^{17}O$ is observed for air samples where the potential temperature is higher, about 420 K and above (Figure 9). At these potential temperatures, mixing processes become more significant and the air inside the anticyclone is exported vertically and horizontally into the surrounding stratosphere (von Hobe et al., 2021; Ma et al., 2022). This enhanced mixing apparently causes the diminished slope for the N_2O and $\Delta'^{17}O$ correlation plot (Figure 4) and also a very scattered three isotope plot (Figure 5). Up to a potential temperature of 400 K to 415 K the strong isolation of air inside the ASMA prevents significant mixing of the stratospheric air into the predominately tropospheric inner cyclone (von Hobe et al., 2021)(von Hobe et al., 2021; Vogel et al., 2024). Consequently, the N_2O-$\Delta'^{17}O$ correlation slope of the lowermost stratospheric StratoClim samples agrees with the ones for CARIBIC samples and previously published measurements.
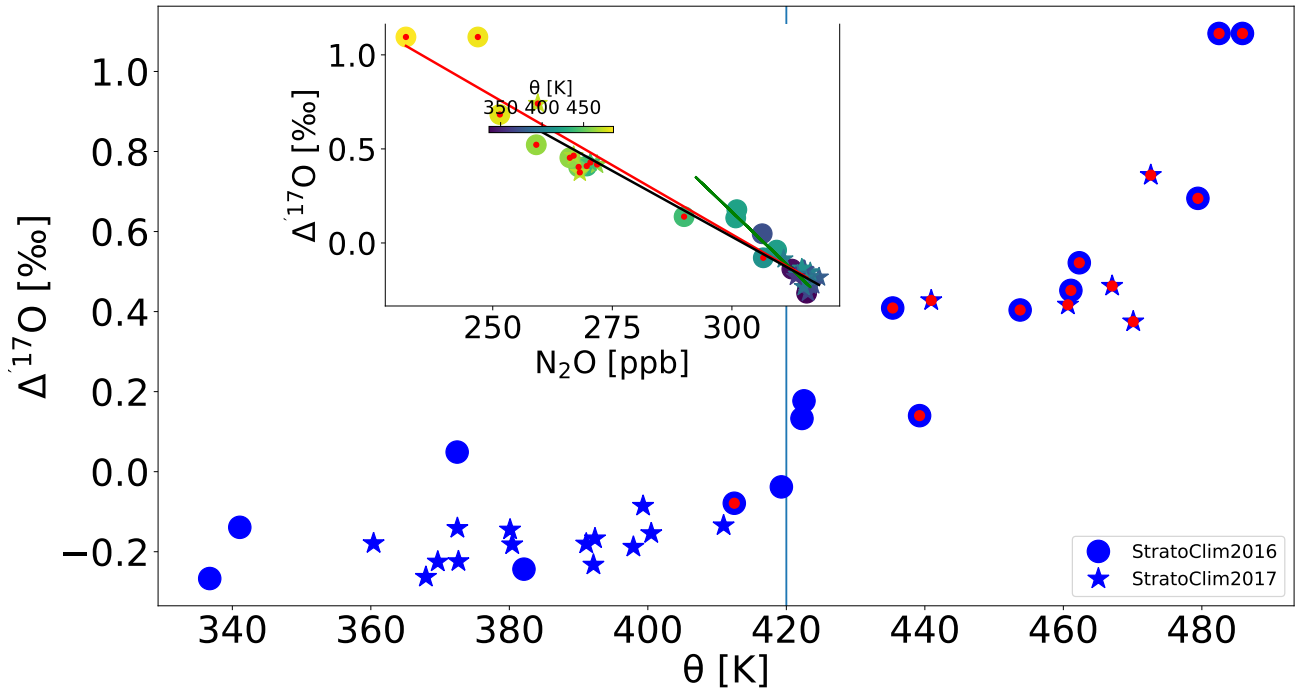
Figure 9. Correlation between $\Delta'^{17}O$ and potential temperature for StratoClim samples. The inset shows the N_2O-$\Delta'^{17}O$ correlation of StratoClim samples from Figure 4. The color bar for the inset is potential temperature. The data points marked in red indicate those with a low N_2O-$\Delta^{17}O$ correlation slope.
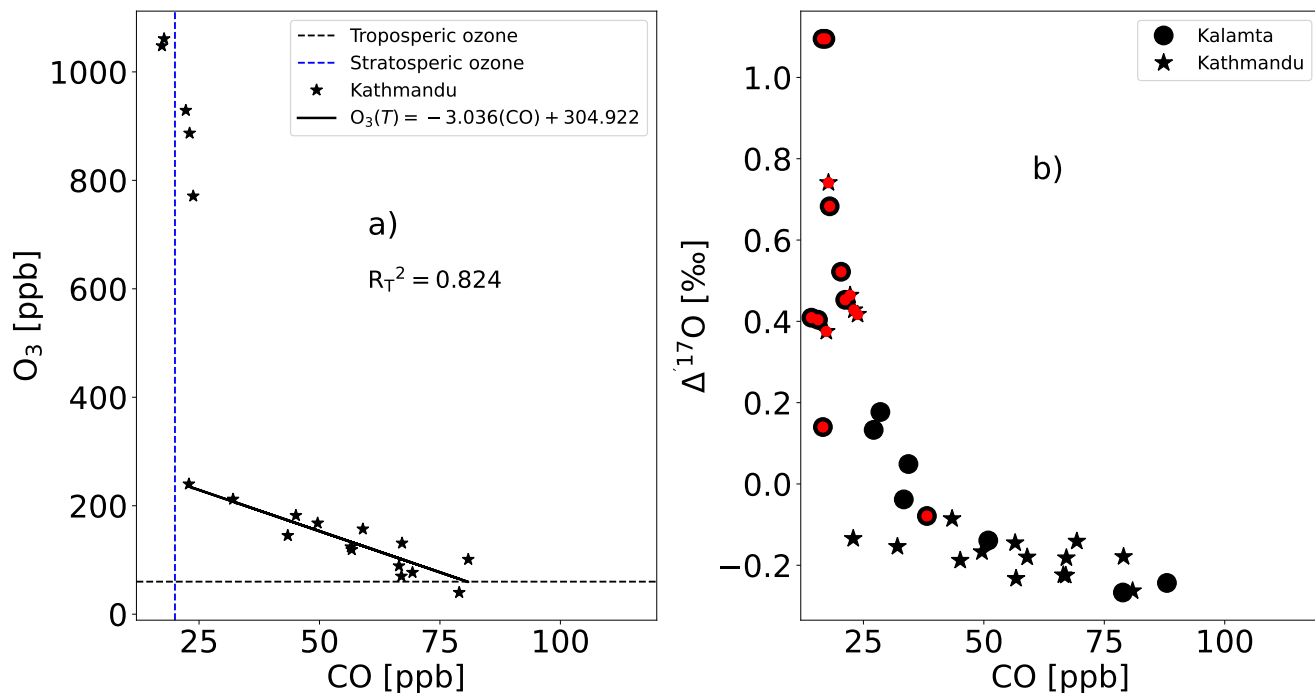
Figure 10. a) The correlation of two short-lived gases, ozone vs CO for Kathmandu samples, b) Correlation of $\Delta'^{17}O$ with CO for both Kalamata and Katmandu samples. The data points marked in red indicate those with a low N_2O-$\Delta^{17}O$ correlation slope.

5 Implication for troposphere and stratosphere exchange and surface emissions of CO_2

Air samples from the upper troposphere and lower stratosphere are well suited for studying stratosphere-troposphere exchange (Olsen et al., 2001). We used CARIBIC samples with $\Delta'^{17}O(CO_2) > -0.2$ ‰ , because for this group $\Delta'^{17}O(CO_2)$ and N_2O have a very compact relationship with a slope of -0.024 $\pm$ 0.0002 ‰ ppb^{-1}, despite the air samples being collected at different latitudes, seasons, and years (see Table S1, Figure 1 and Figure 3). The $\Delta'^{17}O(CO_2)$: N_2O correlation slope is similar to the values reported in the previous measurements (Boering et al., 2004b; Wiegel et al., 2013; Kawagucci et al., 2008). However, the uncertainty of the correlation slope is ten times smaller than in previous measurements (see Garofalo et al. (2019) for a detailed summary), and the new data confirm that the correlation actually extends down to the troposphere. Using the net vertical flux of N_2O (which is equal to the global N_2O loss rate, 13.43 TgNyr^{-1} $\pm$ 3 % (Prather et al., 2023); see also (Tian et al., 2020)), the global mean net flux of $\Delta'^{17}O(CO_2)$ is 51.3 $\pm$ 1.6 ‰PgCyr^{-1}. This estimate aligns well with previous numerical model calculations (Liang et al., 2008) and falls within the range reported previously using a similar approach (Boering et al., 2004b; Garofalo et al., 2019; Wiegel et al., 2013; Kawagucci et al., 2008), but the uncertainty in our estimate is much lower than the 10 to 20 ‰PgCyr^{-1} uncertainty reported in the previous studies (Garofalo et al., 2019). The relatively precise estimate of the net

$\Delta'^{17}O(CO_2)$ flux from the stratosphere to the troposphere results from the improved precision of $\Delta'^{17}O(CO_2)$ measurements (see Figure 8) and the reduced uncertainty in the global N_2O loss rate (3 % vs. 25 %).

495   Using the mass balance model described in section 2.6 (see equation 8), we estimated a terrestrial flux of 749 ± 93 PgC/year. This estimate falls within the range,near the upper range of values, reported by previous studies (200 - 817 PgC/year) (Ciais et al., 1997a, b; Cuntz et al., 2003b, a; Farquhar et al., 1993; Liang et al., 2017b; Welp, 2011). The surface flux, which is the sum of terrestrial and ocean fluxes, is 829 ± 93 PgC/year (see Figure 11). This value is consistent with the range reported by Welp et al. (2008) using $\delta^{18}O$ of CO_2. The corresponding surface turnover time of CO_2 is 0.98 ± 0.1 years, also within the

500   range of previous estimates (i.e., 0.4 to 2.8 years) (Liang et al., 2017b, 2023; Laskar et al., 2019; Welp et al., 2011; Farquhar et al., 1993; Ciais et al., 1997a; Cuntz et al., 2003b) (see Figure 11). As shown in Figure 11, the estimated surface flux and turnover time of CO_2 are sensitive to the $\Delta'^{17}O(CO_2)$ value in the upper troposphere. A higher $\Delta'^{17}O(CO_2)$ value in the upper troposphere results in a lower surface flux and a longer CO_2 turnover time. ~~A detailed sensitivity analysis is provided in the supplementary material.~~ The GPP value is 211 ± 26 PgC/year, which is in good agreement with the estimates (200 PgC/year)

505   by Liang et al. (2023) and Hofmann et al. (2017) using $\Delta'^{17}O(CO_2)$ and higher than the estimate (150-175 PgC/year) by Welp et al. (2008) using $\delta^{18}O$ of CO_2. These estimates are very sensitive to the assumed c_m/c_a ratio, the degree of equilibration (Cuntz, 2011; Farquhar et al., 1993) and the soil invasion flux (Wingate et al., 2009). For example, increasing the c_m/c_a ratio by 0.05 (c_m/c_a = 0.7) decreases the GPP from 212 PgC/year to 189 PgC/year. Conversely, decreasing the c_m/c_a ratio by 0.05 (c_m/c_a = 0.6) will increase the GPP from 212 to 234 PgC/year. A detailed sensitivity analysis is provided in the supplementary

510   material. Although the approach involves a number of assumptions as detailed in the methods section, it has the potential to be a valuable tool for quantifying and refining gross fluxes (Hoag et al., 2005; Koren et al., 2019). This will be especially true when more measurements become available from the lower stratosphere/upper troposphere and troposphere/surface. Additionally, understanding the effects of various processes on $\Delta'^{17}O(CO_2)$, such as soil invasion, and taking into account inter-laboratory calibration scale differences (Adnew and Röckmann, 2022; Liang et al., 2023) and proper model assimilation (Koren et al.,

515   2019), will further enhance its effectiveness.

6   Conclusions

<u>High-precision measurements of $\Delta'^{17}O(CO_2)$ enable the identification of mixing, transport, and chemical processes in the stratosphere.</u> Through the analysis of CARIBIC samples, this study showed that the N_2O-$\Delta'^{17}O(CO_2)$ correlation reported previously from stratospheric samples extends down to the tropopause. Using the N_2O-$\Delta'^{17}O(CO_2)$ correlation slope of

520   CARIBIC samples, we estimated the net mean $\Delta'^{17}O(CO_2)$ flux from the stratosphere to the troposphere to be 51.3 ± 1.6 ‰PgCyr^{-1}. Notably, no significant spatial or hemispheric variability was observed in $\Delta'^{17}O(CO_2)$ values for the upper tropospheric samples collected during the CARIBIC program. The new measurements can be used in a mass balance approach to estimate that the surface turnover time of CO_2 is approximately 1 year, and the GPP is estimated to between 185 to 237 PgC/year.
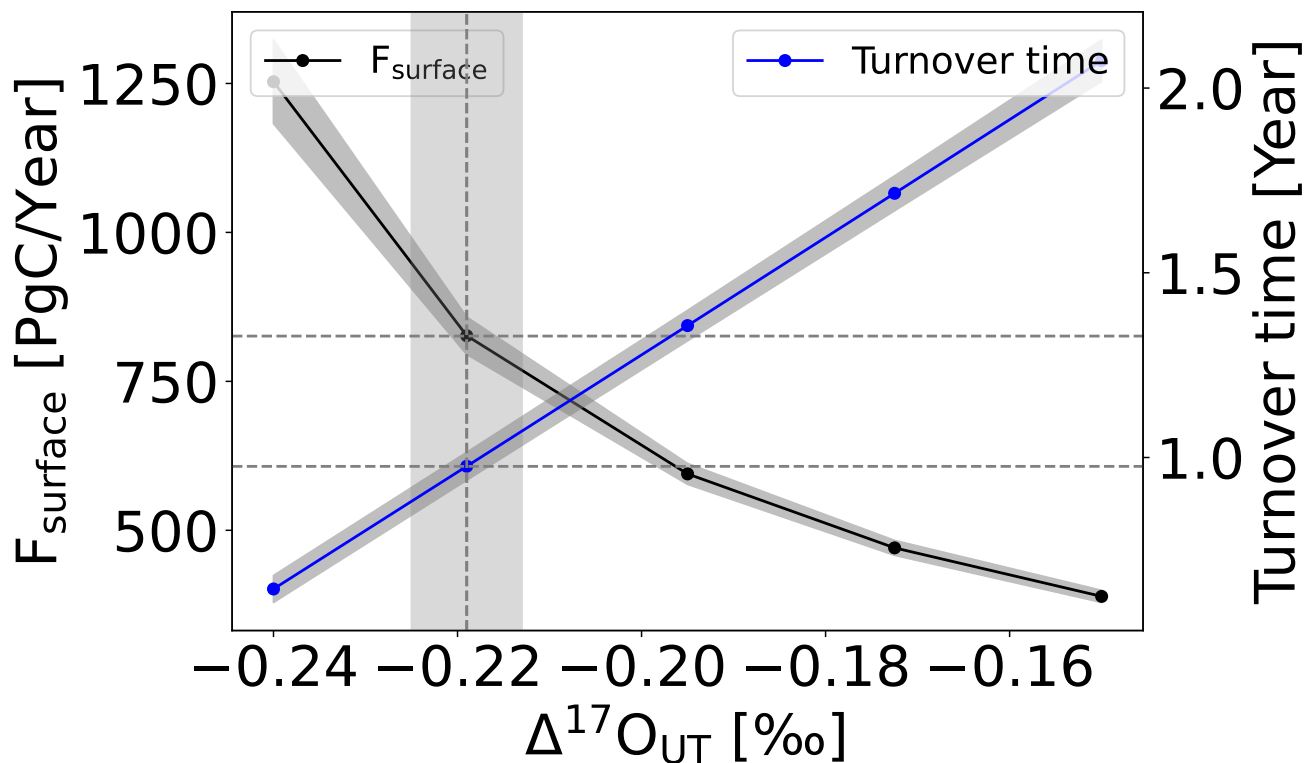
Figure 11. Surface flux of CO_2 (F_{Surf}, left axis) and the oxygen isotope turnover time of CO_2 (left axis) as a function of the $\Delta'^{17}O_{UT}$ value of upper tropospheric CO_2. The solid line indicates our best estimates of F_{Surf} and the oxygen isotope turnover time of CO_2 and the shaded area is the corresponding uncertainty calculated using error propagation.

525   In contrast, StratoClim samples showed a much lower N_2O-$\Delta'^{17}O$ slope compared to CARIBIC samples and previous studies. This deviation is attributed to the increased mixing/eddy diffusion due to ASMA. N_2O-$\Delta'^{17}O$ slope may thus be a direct measurable tracer for the intensity of vertical mixing in the UTLS region.

Author contributions. GAA: Conceptualization; data curation; formal analysis; investigation; methodology; software, visualization; Writing
530 - original draft; Writing - review & editing, GK:investigation, Writing - review & editing, NM: data curation, Writing - review & editing, SG:investigation, MK: data curation, Writing - review & editing, TR: Conceptualization; investigation; methodology, Writing - review & editing

References

Adcock, K. E., Fraser, P. J., Hall, B. D., Langenfelds, R. L., Lee, G., Montzka, S. A., Oram, D. E., Röckmann, T., Stroh, F., Sturges, W. T., et al.: Aircraft-based observations of ozone-depleting substances in the upper troposphere and lower stratosphere in and above the Asian summer monsoon, Journal of Geophysical Research: Atmospheres, 126, e2020JD033 137, 2021.

Adnew, G. A.: The effect of photosynthetic gas exchange on $\Delta 17O$ of atmospheric CO2, PhD thesis, pp. 1–174, https://doi.org/10.33540/412, 2020.

Adnew, G. A. and Röckmann, T.: Urgent need for $\Delta^{17}O$ (CO_2) standardization. The 21st expert meeting on Greenhouse gas measurement techniques (GGMT), Wageningen, The Netherlands, 2022.

Adnew, G. A., Hofmann, M. E. G., Paul, D., Laskar, A., Surma, J., Albrecht, N., Pack, A., Schwieters, J., Koren, G., Peters, W., and Röckmann, T.: Determination of the triple oxygen and carbon isotopic composition of CO2 from atomic ion fragments formed in the ion source of the 253 Ultra High-Resolution Isotope Ratio Mass Spectrometer, Rapid Commun Mass Spectrom., 33, 17, 2019.

Adnew, G. A., Pons, T. L., Koren, G., Peters, W., and Röckmann, T.: Leaf-scale quantification of the effect of photosynthetic gas exchange on $\Delta 17O$ of atmospheric CO2, Biogeosciences Discuss., 2020, 1–37, https://doi.org/10.5194/bg-2020-91, 2020a.

Adnew, G. A., Pons, T. L., Koren, G., Peters, W., and Röckmann, T.: Leaf-scale quantification of the effect of photosynthetic gas exchange on Δ 17 O of atmospheric CO 2, Biogeosciences, 17, 3903–3922, 2020b.

Adnew, G. A., G.Koren, Ziegler, M., and Röckmann, T.: Leaf scale quantification of the effect of photosynthetic gas exchange on $\Delta 47$ of CO2, Sci. Rep., 11, 14 023, https://doi.org/10.1038/s41598-021-93092-0, 2021.

Adnew, G. A., Workman, E., Janssen, C., and Röckmann, T.: Temperature dependence of isotopic fractionation in the CO2-O2 isotope exchange reaction, Rapid Communications in Mass Spectrometry, p. e9301, 2022.

Adnew, G. A., Pons, T. L., Koren, G., Peters, W., and Röckmann, T.: Exploring the potential of $\Delta 17O$ in CO2 for determining mesophyll conductance, Plant Physiology, p. kiad173, 2023.

Alexander, B., Vollmer, M., Jackson, T., Weiss, R., and Thiemens, M.: Stratospheric CO2 isotopic anomalies and SF6 and CFC tracer concentrations in the Arctic polar vortex, Geophysical Research Letters, 28, 4103–4106, 2001.

Angert, A., Rachmilevitch, S., Barkan, E., and Luz, B.: Effects of photorespiration, the cytochrome pathway, and the alternative pathway on the triple isotopic composition of atmospheric O2, Global Biogeochemical Cycles, 1, 1030, 2003.

Angert, A., Cappa, C. D., and DePaolo, D. J.: Kinetic 17O effects in the hydrologic cycle: Indirect evidence and implications, Geochim. Cosmochim. Acta, 68, 3487–3495, 2004.

Annamalai, H. and Slingo, J.: Active/break cycles: Diagnosis of the intraseasonal variability of the Asian summer monsoon, Climate Dynamics, 18, 85–102, 2001.

Appenzeller, C., Holton, J. R., and Rosenlof, K. H.: Seasonal variation of mass transport across the tropopause, Journal of Geophysical Research: Atmospheres, 101, 15 071–15 078, 1996.

Assonov, S., Taylor, P., and Brenninkmeijer, C.: A system for high-quality CO2 isotope analyses of air samples collected by the CARIBIC Airbus A340-600, Rapid Communications in Mass Spectrometry, 23, 1347–1363, 2009a.

Assonov, S. S., Brenninkmeijer, C. A. M., Koeppel, C., and Röckmann, T.: CO2 isotope analyses using large air samples collected on intercontinental flights by the CARIBIC Boeing 767, Rapid Commun. Mass Spctrom., 23, 822–830, 2009b.

Assonov, S. S., Brenninkmeijer, C. A. M., Schuck, T. J., and Taylor, P.: Analysis of 13C and 18O isotope data of CO2 in CARIBIC aircraft samples as tracers of upper troposphere/lower stratosphere mixing and the global carbon cycle, Atoms. Chem Phys., 10, 8575–8599, 2010.

580   Assonov, S. S., Brenninkmeijer, C. A. M., Schuck, T., and Umezawa, T.: N2O as a tracer of mixing stratospheric and tropospheric air based on CARIBIC data with applications for CO2, Atmos. Environ., 79, 769–779, 2013.

Barkan, E. and Luz, B.: High precision measurements of 17O/16O and 18O/16O ratios in H2O, Rapid Comm. Mass Spectrom., 19, 3737–3742, https://doi.org/10.1002/rcm.2250, 2005.

Barkan, E. and Luz, B.: Diffusivity fractionations of H216O/H217O and H216O/H218O in air and their implications for isotope hydrology,

585   RAPID COMMUN MASS SP, 21, 6, 2007.

Barkan, E. and Luz, B.: High-precision measurements of 17O/16O and 18O/16O ratios in CO2, Rapid Commun. Mass. Sp., 26, 2733–2738, https://doi.org/10.1002/rcm.6400, 2012.

Barkan, E., Musan, I., and Luz, B.: High-precision measurements of δ17O and 17O-excess of NBS19 and NBS18, Rapid Commun. Mass. Sp., 29, 2219–2224, https://doi.org/10.1002/rcm.7378, 2015.

590   Boering, K., Jackson, T., Hoag, K., Cole, A., Perri, M., Thiemens, M., and Atlas, E.: Observations of the anomalous oxygen isotopic composition of carbon dioxide in the lower stratosphere and the flux of the anomaly to the troposphere, Geophysical Research Letters, 31, 2004a.

Boering, K. A., Jackson, T., Hoag, K. J., Cole, A. S., Perri, M. J., Thiemens, M., and Atlas, E.: Observations of the anomalous oxygen isotopic composition of carbon dioxide in the lower stratosphere and the flux of the anomaly to the troposphere, Geophys. Res. Lett., 31,

595   2004b.

Bottinga, Y. and Craig, H.: Oxygen isotope fractionation between CO2 and water, and the isotopic composition of marine atmospheric CO2, Earth Planet Sc. Lett., 5, 10, 1968.

Brenninkmeijer, C. and Röckmann, T.: Russian doll type cryogenic traps: Improved design and isotope separation effects, Analytical chemistry, 68, 3050–3053, 1996.

600   Brenninkmeijer, C., Kraft, P., and Mook, W.: Oxygen isotope fractionation between CO2 and H2O, Chemical Geology, 41, 181–190, 1983.

Brenninkmeijer, C., Lowe, D., Manning, M., Sparks, R., and Van Velthoven, P.: The 13C, 14C, and 18O isotopic composition of CO, CH4, and CO2 in the higher southern latitudes lower stratosphere, Journal of Geophysical Research: Atmospheres, 100, 26 163–26 172, 1995.

Brenninkmeijer, C., Crutzen, P., Fischer, H., Güsten, H., Hans, W., Heinrich, G., Heintzenberg, J., Hermann, M., Immelmann, T., Kersting, D., et al.: CARIBIC—Civil aircraft for global measurement of trace gases and aerosols in the tropopause region, Journal of Atmospheric

605   and Oceanic Technology, 16, 1373–1383, 1999.

Brenninkmeijer, C. A.: Robust, high-efficiency, high-capacity cryogenic trap, Analytical Chemistry, 63, 1182–1184, 1991.

Brenninkmeijer, C. A.: Measurement of the abundance of 14CO in the atmosphere and the 13C/12C and 18O/16O ratio of atmospheric CO with applications in New Zealand and Antarctica, Journal of Geophysical Research: Atmospheres, 98, 10 595–10 614, 1993.

Brunamonti, S., Jorge, T., Oelsner, P., Hanumanthu, S., Singh, B. B., Kumar, K. R., Sonbawne, S., Meier, S., Singh, D., Wienhold, F. G.,

610   et al.: Balloon-borne measurements of temperature, water vapor, ozone and aerosol backscatter on the southern slopes of the Himalayas during StratoClim 2016–2017, Atmospheric Chemistry and Physics, 18, 15 937–15 957, 2018.

Cairo, F., Pommereau, J.-P., Law, K. S., Schlager, H., Garnier, A., Fierli, F., Ern, M., Streibel, M., Arabas, S., Borrmann, S., et al.: An introduction to the SCOUT-AMMA stratospheric aircraft, balloons and sondes campaign in West Africa, August 2006: rationale and roadmap, Atmospheric chemistry and physics, 10, 2237–2256, 2010.

615   Cao, X. and Liu, Y.: Equilibrium mass-dependent fractionation relationships for triple oxygen isotopes, Geochim. Cosmochim. Acta., 75, 7435–7445, 2011.

Cernusak, L. A., Barbour, M. M., Arndt, S. K., Cheesman, A. K., English, N. B., Feild, T. S., Helliker, B. R., Holloway-Phillips, M. M., Holtum, J. A., Kahmen, A., McInerney, F. A., Munksgaard, N. C., Simonin, K. A., Song, X., Stuart-Williams, H., West, J. B., and Farquhar, G. D.: Stable isotopes in leaf water of terrestrial plants, Plant Cell Environ., 39, 1087–1102, https://doi.org/10.1111/pce.12703, 2016.

620   Ciais, P., Tans, P. P., Trolier, M., White, J. W. C., and Francey, R. J.: A large northern hemisphere terrestrial CO2 sink indicated by the 13C/12C ratio of atmospheric CO2 , Science, 269, 4, 1995.

Ciais, P., Denning, A. S., Tans, P. P., Berry, J. A., Randall, D. A., Collatz, G. J., Sellers, P. J., White, J. W., Trolier, M., Meijer, H. A., et al.: A three-dimensional synthesis study of $\delta 18O$ in atmospheric CO2: 1. Surface fluxes, Journal of Geophysical Research: Atmospheres, 102, 5857–5872, 1997a.

625   Ciais, P., Tans, P. P., Denning, A. S., Francey, R. J., Trolier, M., Meijer, H. A., White, J. W., Berry, J. A., Randall, D. A., Collatz, G. J., et al.: A three-dimensional synthesis study of $\delta 18O$ in atmospheric CO2: 2. Simulations with the TM2 transport model, Journal of Geophysical Research: Atmospheres, 102, 5873–5883, 1997b.

Cousins, A. B., Badger, M. R., and Caemmerer, S. v.: Carbonic anhydrase and its influence on carbon isotope discrimination during C4 photosynthesis. Insights from antisense RNA in Flaveria bidentis, Plant Physiol., 141, 232–242, 2006.

630   Cuntz, M.: A dent in carbon's gold standard, Nature, 477, 547–548, 2011.

Cuntz, M., Ciais, P., Hoffmann, G., Allison, C. E., Francey, R. J., Knorr, W., Tans, P. P., White, J. W., and Levin, I.: A comprehensive global three-dimensional model of $\delta 18O$ in atmospheric CO2: 2. Mapping the atmospheric signal, Journal of Geophysical Research: Atmospheres, 108, 2003a.

Cuntz, M., Ciais, P., Hoffmann, G., and Knorr, W.: A comprehensive global three-dimensional model of $\delta 18O$ in atmospheric CO2: 1.
635   Validation of surface processes, Journal of Geophysical Research: Atmospheres, 108, 2003b.

Dai, A.: Recent climatology, variability, and trends in global surface humidity, J. Clim., 19, 17, 2006.

Engel, A., Rigby, M., Burkholder, J. B., Fernandez, R. P., Froidevaux, L., Hall, B. D., Hossaini, R., Saito, T., Vollmer, M. K., and Yao, B.: Update on ozone-depleting substances (ODSs) and other gases of interest to the Montreal Protocol, 2019.

Farquhar, G. D. and Lloyd, J.: Carbon and oxygen isotope effects in the exchange of carbon dioxide between terrestrial plants and the
640   atmosphere, Acadamic Press Inc, London, 1993.

Farquhar, G. D., Lloyd, J., Taylor, J. A., Flanagan, L. B., Syvertsen, J. P., Hubick, K. T., Wong, S. C., and Ehleringer, J. R.: Vegetation effects on the isotope composition of oxygen in atmospheric CO2, Nature, 363, 439–443, 1993.

Francey, R. J. and Tans, P. P.: Latitudinal variation in oxygen-18 of atmospheric CO2, Nature, 327, 495–497, 1987.

Friedli, H. and Siegenthaler, U.: Influence of N2O on isotope analyses in CO2 and mass-spectrometric determination of N2O in air samples,
645   Tellus B, 40, 129–133, 1988.

Gamo, T., Tsutsumi, M., Sakai, H., Nakazawa, T., Machida, T., Honda, H., and Itoh, T.: Long-term monitoring of carbon and oxygen isotope ratios of stratospheric CO2 over Japan, Geophysical research letters, 22, 397–400, 1995.

Gan, K. S., Wong, S. C., Yong, J. W. H., and Farquhar, G. D.: 18O spatial patterns of vein xylem water, leaf water, and dry matter in cotton leaves, Plant Physiol., 130, 13, 2002.

650   Garny, H. and Randel, W.: Dynamic variability of the Asian monsoon anticyclone observed in potential vorticity and correlations with tracer distributions, Journal of Geophysical Research: Atmospheres, 118, 13–421, 2013.

Garofalo, L., Kanu, A., Hoag, K. J., and Boering, K. A.: The effects of stratospheric chemistry and transport on the isotopic compositions of long-lived gases measured at Earth's surface, Advances in Atmospheric Chemistry: Volume 2: Organic Oxidation and Multiphase Chemistry, pp. 529–587, 2019.

655 Hayles, J. A. and Killingsworth, B. A.: Constraints on triple oxygen isotope kinetics, Chemical Geology, 589, 120 646, 2022.

Hayles, J. A., Cao, X., and Bao, H.: The statistical mechanical basis of the triple isotope fractionation relationship, Geochem. Perspect. Lett, 3, 1–11, 2017.

Helliker, B. R. and Ehleringer, J. R.: Establishing a grassland signature in veins: 18O in the leaf water of C3 and C4 grasses, PNAS, 97, 7894–7898, 2000.

660 Hoag, K. J., Still, C. J., and Fung, I. Y.: Triple oxygen isotope composition of tropospheric carbon dioxide as a tracer of terrestrial gross carbon fluxes, Geophys. Res. Lett., 32, https://doi.org/10.1029/2004gl021011, 2005.

Hofmann, M. E. G., Horváth, B., and Pack, A.: Triple oxygen isotope equilibrium fractionation between carbon dioxide and water, Earth Planet Sci Lett., 319, 159–164, 2012.

Hofmann, M. E. G., Horváth, B., Schneider, L., Peters, W., Schützenmeister, K., and Pack, A.: Atmospheric measurements of Δ17O
665 in CO2 in Göttingen, Germany reveal a seasonal cycle driven by biospheric uptake, Geochim. Cosmochim. Ac., 199, 143–163, https://doi.org/10.1016/j.gca.2016.11.019, 2017.

Holton, J. R., Haynes, P. H., McIntyre, M. E., Douglass, A. R., Rood, R. B., and Pfister, L.: Stratosphere-troposphere exchange, Reviews of geophysics, 33, 403–439, 1995.

Horváth, B., Hofmann, M., and Pack, A.: On the triple oxygen isotope composition of carbon dioxide from some combustion processes,
670 Geochimica et Cosmochimica Acta, 95, 160–168, 2012.

Kaiser, J.: Reformulated 17O correction of mass spectrometric stable isotope measurements in carbon dioxide and a critical appraisal of historic 'absolute' carbon and oxygen isotope ratios, Geochimica et Cosmochimica Acta, 72, 22, https://doi.org/10.1016/j.gca.2007.12.011, 2008.

Kaiser, J., Engel, A., Borchers, R., and Röckmann, T.: Probing stratospheric transport and chemistry with new balloon and aircraft observa-
675 tions of the meridional and vertical N 2 O isotope distribution, Atmospheric Chemistry and Physics, 6, 3535–3556, 2006.

Kawagucci, S., Tsunogai, U., Kudo, S., Nakagawa, F., Honda, H., Aoki, S., Nakazawa, T., and Gamo, T.: An analytical system for determining δ17O in CO2 using continuous flow-isotope ratio MS, Anal. Chem, 77, 5, 2005.

Kawagucci, S., Tsunogai, U., Kudo, S., Nakagawa, F., Honda, H., Aoki, S., Nakazawa, T., Tsutsumi, M., and Gamo, T.: Long-term observation of mass-independent oxygen isotope anomaly in stratospheric CO2, Atmos. Chem. Phys., 8, 8, 2008.

680 Koren, G., Schneider, L., Velde, I. d., Schaik, E. v., Gromov, S. S., Adnew, G. A., D.J.Mrozek, Hofmann, M. E. D., Liang, M.-C., Mahata, S., Bergamaschi, P., Laan-Luijkx, I. T. v. d., Krol, M. C., Röckmann, T., and Peters, W.: Global 3-D Simulations of the Triple Oxygen Isotope Signature Δ17O in Atmospheric CO2, J. Geophys. Res. Atmos., 124, 28, 2019.

Krol, M., De Bruine, M., Killaars, L., Ouwersloot, H., Pozzer, A., Yin, Y., Chevallier, F., Bousquet, P., Patra, P., Belikov, D., et al.: Age of air as a diagnostic for transport timescales in global models, Geoscientific Model Development, 11, 3109–3130, 2018.

685 Lämmerzahl, P., Röckmann, T., and Brenninkmeijer, C. A. M.: Oxygen isotope composition of stratospheric carbon dioxide, Geophys. Res. Lett., 29, https://doi.org/10.1029/2001gl014343, 2002.

Lan, X., Thoning, K. W., and Dlugokencky, E. J.: Trends in globally-averaged CH4, N2O, and SF6 determined from NOAA Global Monitoring Laboratory measurements, Version 2024-08, https://doi.org/10.15138/P8XG-AA10, 15, 753–759, 2024.

Landais, A., Barkan, E., Yakir, D., and Luz, B.: The triple isotopic composition of oxygen in leaf water, Geochim. Cosmochim. Ac., 70,
690 4105–4115, https://doi.org/10.1016/j.gca.2006.06.1545, 2006.

Landais, A., Yakir, D., Barkan, E., and Luz, B.: The triple isotopic composition of oxygen in leaf water and its implications for quantifying biosphere productivity, Terrestrial Ecology, 1, 111–125, 2007.

Laskar, A. H., Mahata, S., and Liang, M.-C.: Identification of anthropogenic CO2 using triple oxygen and clumped isotopes, Environ. Sci. Technol., 50, 18, https://doi.org/10.1021/acs.est.6b02989, 2016.

695 Laskar, A. M., Mahata, S., Bhattacharya, S. K., and Liang, M.-C.: Triple oxygen and clumped isotope compositions of CO2 in the middle troposphere , Earth and Space Science, 6, 1205–1219, 2019.

Levin, I., Allison, C., Brand, W., Conway, Delmotte, M., Facklam, C., Francey, R., Hammer, S., Huang, L., Jordan, A., Langenfelds, R., Machida, T., Meijer, H., Mukai, H., Neubert, R., Sabasch, M., Schmidt, M., Steele, P., Steinberg, B., Ramonet, M., Rothe, M., Vaughn, B., , and Worthy, D.: Five Years of International Flask Intercomparison (Sausage Flask ICP) 2002– 2007,14th WMO/IAEA Meeting of

700 Experts on Carbon Dioxide, Other Greenhouse Gases and Related Tracers Measurement Techniques, GAW Report No, 194, 330, 2007.

Liang, M.-C. and Mahata, S.: Oxygen anomaly in near surface carbon dioxide reveals deep stratospheric intrusion, Sci. Rep., 5, 11 352, https://doi.org/10.1038/srep11352, 2015.

Liang, M.-C., Blake, G. A., Lewis, B. R., and Yung, Y. L.: Oxygen isotopic composition of carbon dioxide in the middle atmosphere, Proceedings of the National Academy of Sciences, 104, 21–25, 2007a.

705 Liang, M.-C., Geoffrey, A. B., Brenton, R. L., and Yung, Y. L.: Oxygen isotopic composition of carbon dioxide in the middle atmosphere, PNAS, 104, 5, 2007b.

Liang, M.-C., Blake, G. A., and Yung, Y. L.: Seasonal cycle of C16O16O, C16O17O, and C16O18O in the middle atmosphere: Implications for mesospheric dynamics and biogeochemical sources and sinks of CO2 , J. Geophys. Res. Atmos., 113, D12, 2008.

Liang, M.-C., Mahata, S., Laskar, A. H., and Bhattacharya, S. K.: Spatiotemporal variability of oxygen isotope anomaly in near surface air

710 CO2 over urban, semi-urban and ocean areas in and around Taiwan, Aerosol Air Qual. Res., 17, 24, 2017a.

Liang, M.-C., Mahata, S., Laskar, A. H., Thiemens, M. H., and Newman, S.: Oxygen isotope anomaly in tropospheric CO2 and implications for CO2 residence time in the atmosphere and gross primary productivity, Sci Rep, 7, 13 180, https://doi.org/10.1038/s41598-017-12774-w, 2017b.

Liang, M.-C., Laskar, A. H., Barkan, E., Newman, S., Thiemens, M. H., and Rangarajan, R.: New constraints of terrestrial and oceanic global

715 gross primary productions from the triple oxygen isotopic composition of atmospheric CO2 and O2, Scientific Reports, 13, 2162, 2023.

Luz, B. and Barkan, E.: Variations of 17O/16O and 18O/16O in meteoric waters , Geochim. Cosmochim. Ac., 74, 10, 2010.

Luz, B., Barkan, E., Bender, M. L., Thiemens, M. K., and Boering, K. A.: Triple-isotope composition of atmospheric oxygen as a tracer of biosphere productivity , Nature, 400, 3, 1999.

Lyons, J. R.: Transfer of mass-independent fractionation in ozone to other oxygen-containing radicals in the atmosphere, Geophys. Res.

720 Lett., 28, 3231–3234, https://doi.org/10.1029/2000gl012791, 2001.

Ma, D., Bian, J., Li, D., Bai, Z., Li, Q., Zhang, J., Wang, H., Zheng, X., Hurst, D. F., and Vömel, H.: Mixing characteristics within the tropopause transition layer over the Asian summer monsoon region based on ozone and water vapor sounding data, Atmospheric Research, 271, 106 093, 2022.

Matsuhisa, Y., Goldsmith, J. R., and Clayton, R. N.: Mechanisms of hydrothermal crystallization of quartz at 250oC and 15 kbar , Geochim.

725 Cosmochim. Acta, 42, 9, 1978.

Meijer, H. and Li, W.: The use of electrolysis for accurate 17O and 18O isotope measurements in water isotopes, Isotopes Environ. Health Stud., 34, 20, 1998.

Mikkonen, S., Pitkänen, M. R., Nieminen, T., Lipponen, A., Isokääntä, S., Arola, A., and Lehtinen, K. E.: Effects of uncertainties and number of data points on line fitting–a case study on new particle formation, Atmospheric Chemistry and Physics, 19, 12 531–12 543, 2019.

730   Miller, J. B., Yakir, D., White, J. W., and Tans, P. P.: Measurement of 18O/16O in the soil-atmosphere CO2 flux, Global Biogeochemical
          Cycles, 13, 761–774, 1999.

       Mrozek, D. J. et al.: Measurements and interpretation of oxygen isotopes in stratospheric carbon dioxide, Ph.D. thesis, Utrecht University,
          2017.

       Nisbet, E. G., Manning, M., Dlugokencky, E., Fisher, R., Lowry, D., Michel, S., Myhre, C. L., Platt, S. M., Allen, G., Bousquet, P., et al.:
735   Very strong atmospheric methane growth in the 4 years 2014–2017: Implications for the Paris Agreement, Global Biogeochemical Cycles,
          33, 318–342, 2019.

       Olsen, S., McLinden, C., and Prather, M.: Stratospheric N2O–NO y system: Testing uncertainties in a three-dimensional framework, Journal
          of Geophysical Research: Atmospheres, 106, 28 771–28 784, 2001.

       Pan, L. L., Honomichl, S. B., Kinnison, D. E., Abalos, M., Randel, W. J., Bergman, J. W., and Bian, J.: Transport of chemical tracers
740   from the boundary layer to stratosphere associated with the dynamics of the Asian summer monsoon, Journal of Geophysical Research:
          Atmospheres, 121, 14–159, 2016.

       Park, M., Randel, W. J., Emmons, L. K., and Livesey, N. J.: Transport pathways of carbon monoxide in the Asian summer monsoon diagnosed
          from Model of Ozone and Related Tracers (MOZART), Journal of Geophysical Research: Atmospheres, 114, 2009.

       Peylin, P., Ciais, P., Denning, A. S., Tans, P. P., Berry, J. A., and White, J. W.: A 3-dimensional study of δ18O in atmospheric CO2:
745   contribution of different land ecosystems, Tellus B, 51, 25, 1999.

       Piao, S., Sitch, S., Ciais, P., Friedlingstein, P., Peylin, P., Wang, X., Ahlström, A., Anav, A., Canadell, J. G., Cong, N., et al.: Evaluation of
          terrestrial carbon cycle models for their response to climate variability and to CO2 trends, Global change biology, 19, 2117–2132, 2013.

       Plumb, R. A.: Tracer interrelationships in the stratosphere, Reviews of Geophysics, 45, 2007.

       Plumb, R. A. and Ko, M. K.: Interrelationships between mixing ratios of long-lived stratospheric constituents, Journal of Geophysical
750   Research: Atmospheres, 97, 10 145–10 156, 1992.

       Prather, M. J., Froidevaux, L., and Livesey, N. J.: Observed changes in stratospheric circulation: decreasing lifetime of N 2 O, 2005–2021,
          Atmospheric Chemistry and Physics, 23, 843–849, 2023.

       Pupek, M., Assonov, S., Mühle, J., Rhee, T., Oram, D., Koeppel, C., Slemr, F., and Brenninkmeijer, C.: Isotope analysis of hydrocarbons:
          trapping, recovering and archiving hydrocarbons and halocarbons separated from ambient air, Rapid Communications in Mass Spectrom-
755   etry: An International Journal Devoted to the Rapid Dissemination of Up-to-the-Minute Research in Mass Spectrometry, 19, 455–460,
          2005.

       Saugier, B., Roy, J., and Mooney, H. A.: Estimations of global terrestrial productivity, Terrestrial global productivity, pp. 543–557, 2001.

       Shaheen, R., Janssen, C., and Röckmann, T.: Investigations of the photochemical isotope equilibrium between O2, CO2 and O3, Atmos.
          Chem. Phys, 7, 14, 2007.

760   Sirignano, C., Neubert, R. E., and Meijer, H. A.: N2O influence on isotopic measurements of atmospheric CO2, Rapid communications in
          mass spectrometry, 18, 1839–1846, 2004.

       Song, X., Simonin, K. A., Loucos, K. E., and Barbour, M. M.: Modelling non-steady-state isotope enrichment of leaf water in a gas-exchange
          cuvette environment, Plant Cell Environ., 38, 10, 2015.

       Stefanutti, L., Sokolov, L., Balestri, S., MacKenzie, A., and Khattatov, V.: The M-55 Geophysica as a platform for the Airborne Polar
765   Experiment, Journal of Atmospheric and Oceanic Technology, 16, 1303–1312, 1999.

       Stern, L. A., Amundson, R., and Baisden, W. T.: Influence of soils on oxygen isotope ratio of atmospheric CO2, Global Biogeochemical
          Cycles, 15, 753–759, 2001.

Steur, P. M., Scheeren, H. A., Koren, G., Adnew, G. A., Peters, W., and Meijer, H. A.: Interannual variations in the Δ (17 O) signature of atmospheric CO 2 at two mid-latitude sites suggest a close link to stratosphere-troposphere exchange, EGUsphere, 2024, 1–31, 2024.

770 Stocker, T., Qin, D., Plattner, G-K Tignor, M., Allen, S., Boschung, J., Nauels, A., Xia, Y., Bex, V., and Midgley, P.: IPCC, 2013: Climate Change 2013: The Physical Science Basis. Contribution of Working Group I to the Fifth Assessment Report of the Intergovernmental Panel on Climate Change, Cambridge University Press, Cambridge, United Kingdom and New York, NY, USA, p. 1535, 2013.

Thiemens, M. H.: History and Applications of Mass-Independent Isotope Effects, Annu. Rev. Earth Planet. Sci., 34, 62, https://doi.org/10.1146/, 2006.

775 Thiemens, M. H., Jackso, T., Mauersberger, K., Schueler, B., and Morton, J.: Oxygen isotope fractionation in stratospheric CO2, Geophys. Res. Lett., 18, 3, 1991.

Thiemens, M. H., Jackson, T., Zipf, E. C., Erdman, P. W., and van Egmond, C.: Carbon dioxide and oxygen isotope anomalies in the mesosphere and stratosphere, Science, 270, 969–972, 1995a.

Thiemens, M. H., Jackson, T., Zipf, E. D., Erdman, P. W., and Egmond, C. v.: Carbon dioxide and oxygen isotope anomalies in the mesosphere 780 and stratosphere , Science, 270, 969–972, 1995b.

Thiemens, M. H., Jackson, T. L., and Brenninkmeijer, C. A.: Observation of a mass independent oxygen isotopic composition in terrestrial stratospheric CO2, the link to ozone chemistry, and the possible occurrence in the Martian atmosphere, Geophysical Research Letters, 22, 255–257, 1995c.

Thiemens, M. K., Chakraborty, S., and Jackson, T. L.: Decadal Δ17O record of tropospheric CO2: Verification of a stratospheric component 785 in the troposphere, J. Geophys. Res. Atmos., 119, 8, 2014.

Tian, H., Xu, R., Canadell, J. G., Thompson, R. L., Winiwarter, W., Suntharalingam, P., Davidson, E. A., Ciais, P., Jackson, R. B., Janssens-Maenhout, G., et al.: A comprehensive quantification of global nitrous oxide sources and sinks, Nature, 586, 248–256, 2020.

Vogel, B., Günther, G., Müller, R., Grooß, J.-U., and Riese, M.: Impact of different Asian source regions on the composition of the Asian monsoon anticyclone and of the extratropical lowermost stratosphere, Atmospheric chemistry and physics, 15, 13 699–13 716, 2015.

790 Vogel, B., Günther, G., Müller, R., Grooß, J.-U., Afchine, A., Bozem, H., Hoor, P., Krämer, M., Müller, S., Riese, M., et al.: Long-range transport pathways of tropospheric source gases originating in Asia into the northern lower stratosphere during the Asian monsoon season 2012, Atmospheric Chemistry and Physics, 16, 15 301–15 325, 2016.

Vogel, B., Müller, R., Günther, G., Spang, R., Hanumanthu, S., Li, D., Riese, M., and Stiller, G. P.: Lagrangian simulations of the transport of young air masses to the top of the Asian monsoon anticyclone and into the tropical pipe, Atmospheric Chemistry and Physics, 19, 795 6007–6034, 2019.

Vogel, B., Volk, C. M., Wintel, J., Lauther, V., Clemens, J., Grooß, J.-U., Günther, G., Hoffmann, L., Laube, J. C., Müller, R., et al.: Evaluation of vertical transport in ERA5 and ERA-Interim reanalysis using high-altitude aircraft measurements in the Asian summer monsoon 2017, Atmospheric Chemistry and Physics, 24, 317–343, 2024.

von Hobe, M., Ploeger, F., Konopka, P., Kloss, C., Ulanowski, A., Yushkov, V., Ravegnani, F., Volk, C. M., Pan, L. L., Honomichl, S. B., 800 et al.: Upward transport into and within the Asian monsoon anticyclone as inferred from StratoClim trace gas observations, Atmospheric Chemistry and Physics, 21, 1267–1285, 2021.

Welp, L.: Interannual variability in the oxygen isotopes of atmospheric CO2 driven by El Nino Welp, Lisa R.; Keeling, Ralph F.; Meijer, Harro AJ; Bollenbacher, Alane F.; Piper, Stephen C.; Yoshimura, Kei; Francey, Roger J.; Allison, Colin E.; Wahlen, Martin, Nature, 477, 579–582, 2011.

805   Welp, L. R., Lee, X., Kim, K., Griffis, T. J., Billmark, K. A., and Baker, J. M.: δ18O of water vapour, evapotranspiration and the sites of leaf water evaporation in a soybean canopy, Plant, Cell & Environment, 31, 1214–1228, 2008.

Welp, L. R., Keeling, R. F., Meijer, H. A. J., Bollenbacher, A. F., Piper, S. C., Yoshimura, K., Francey, R. J., Allison, C. A., and Wahlen, M.: Interannual variability in the oxygen isotopes of atmospheric CO2 driven by El Niño, Nature, 477, 579–582, https://doi.org/10.1038/nature10421, 2011.

810   Wiegel, A. A., Cole, A. S., Hoag, K. J., Atlas, E. L., Schauffler, S. M., and Boering, K. A.: Unexpected variations in the triple oxygen isotope composition of stratospheric carbon dioxide, PNAS, 110, 17 680–17 685, https://doi.org/10.1073/pnas.1213082110, 2013.

Wingate, L., Ogée, J., Cuntz, M., Genty, B., Reiter, I., Seibt, U., Yakir, D., Maseyk, K., Pendall, E. G., Barbour, M. M., Mortazavi, B., Burlett, R., Peylin, P., Miller, J., Mencuccini, M., Shim, J. H., Hunt, J., and Grace, J.: The impact of soil microorganisms on the global budget of δ18O in atmospheric CO2, PNAS, 106, 4, 2009.

815   Yakir, D.: Oxygen-18 of leaf water: a crossroad for plant-associated isotopic signals, in: Stable isotopes, pp. 147–168, Garland Science, 2020.

Yeung, L. Y., Affek, H. P., Hoag, K. J., Guo, W., Wiegel, A. A., Atlas, E. L., Schauffler, S. M., Okumura, M., Boering, K. A., and Eiler, J. M.: Large and unexpected enrichment in stratospheric 16O13C18O and its meridional variation, Proceedings of the national academy of sciences, 106, 5, 2009.

Young, E. D., Galy, A., and Nagahara, H.: Kinetic and equilibrium mass-dependent isotope fractionation laws in nature and their geochemical

820   and cosmochemical significance, Geochim. Cosmochim. Ac., 66, 9, 2002.

Yung, Y. L., DeMore, W., and Pinto, J. P.: Isotopic exchange between carbon dioxide and ozone via O (1D) in the stratosphere, Geophysical Research Letters, 18, 13–16, 1991a.

Yung, Y. L., DoMore, W. B., and Pinto, J. P.: Isotopic exhange between carbon dioxide and ozone via O (1D) in the stratosphere, Geophys. Res. Lett., 18, 3, 1991b.

825   Yung, Y. L., Lee, A. Y., Irion, F. W., DeMore, W. B., and Wen, J.: Carbon dioxide in the atmosphere: Isotopic exchange with ozone and its use as a tracer in the middle atmosphere, Journal of Geophysical Research: Atmospheres, 102, 10 857–10 866, 1997a.

Yung, Y. L., Lee, A. Y. T., Irion, F. W., DeMore, W. B., and Wen, J.: Carbon dioxide in the atmosphere: Isotopic exchange with ozone and its use as a tracer in the middle atmosphere, J. Geophys. Res., 102, 9, 1997b.